Climate4you update November 2016

Contents:

November 2016 global surface air temperature overview

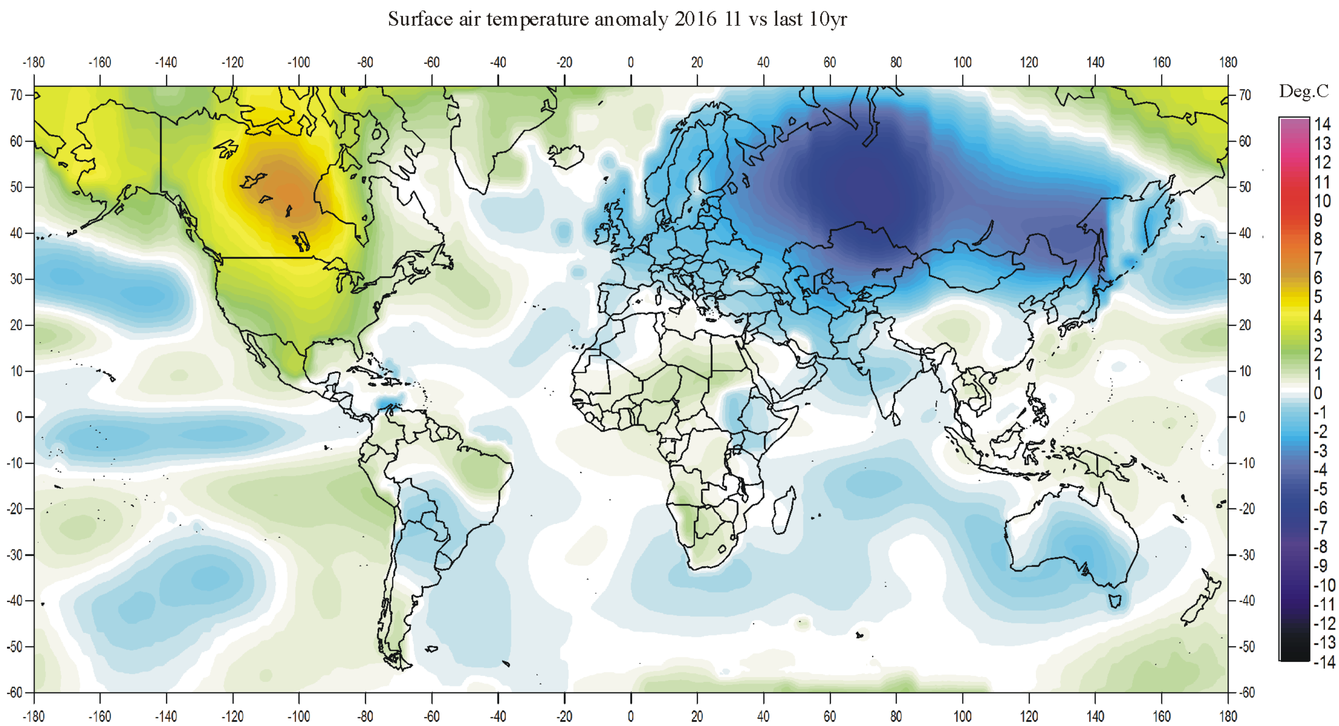

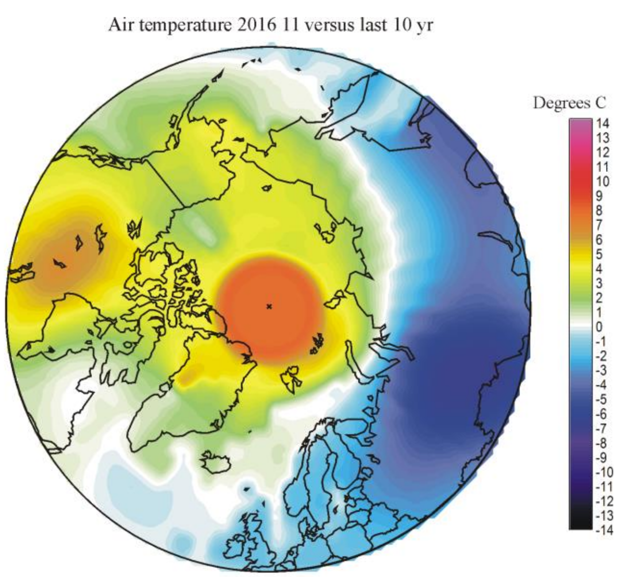

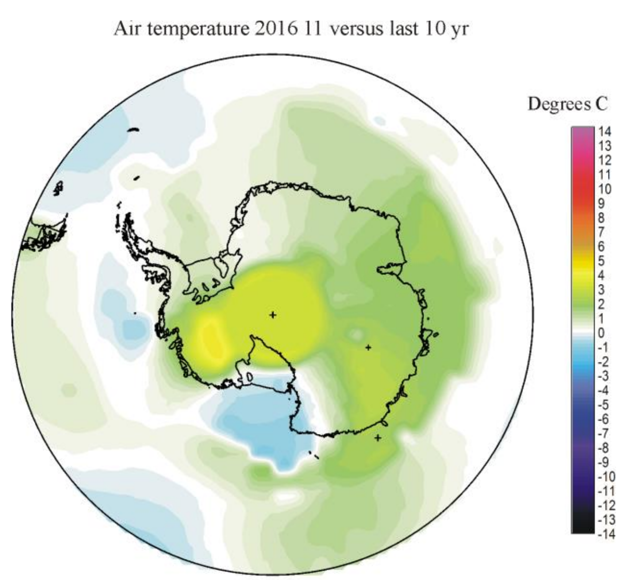

November 2016 surface air temperature compared to the average of the last 10 years. Green-yellow-red colours indicate areas with higher temperature than the 10 year average, while blue colours indicate lower than average temperatures. Data source: [Goddard Institute for Space Studies](#) (GISS) using ERSST_v4 ocean surface temperatures. Please note that both polar regions appear to be affected by an error in the GISS interpolation (see more next page).

Comments to the November 2016 global surface air temperature overview

General: This newsletter contains graphs showing a selection of key meteorological variables for the past month. *All temperatures are given in degrees Celsius*.

In the above maps showing the geographical pattern of surface air temperatures, *the last previous 10 years are used as reference period*.

The rationale for comparing with this recent period instead of the official WMO 'normal' period 1961-1990, is that the latter period is affected by the cold period 1945-1980. Most comparisons with this time period will automatically appear as warm, and it will be difficult to decide if modern surface air temperatures are increasing or decreasing. Comparing instead with the last previous 10 years overcomes this problem and displays the modern dynamics of ongoing change.

In addition, the GISS temperature data used for preparing the above diagrams display distinct temporal instability for data before the turn of the century (see p. 7). Any comparison with the WMO 'normal' period 1961-1990 is therefore influenced by ongoing monthly mainly administrative changes, and not suited as reference. Comparing with the last previous 10 years is more useful.

The different air temperature records have been divided into three quality classes, QC1, QC2 and QC3, respectively, as described on page 7.

In many diagrams shown in this newsletter the thin line represents the monthly global average value, and the thick line indicate a simple running average, in most cases a simple moving 37-month average, nearly corresponding to a three-year average. The 37-month average is calculated from values covering a range from 18 month before to 18 months after, with equal weight given to all individual months.

The year 1979 has been chosen as starting point in many diagrams, as this roughly corresponds to both the beginning of satellite observations and the onset of the late 20th century warming period. However, several of the data series have a much longer record length, which may be inspected in greater detail on www.climate4you.com.

November 2016 global surface air temperatures

General: The average global air temperature was near the average for the last ten years. *The GISS data is probably providing a somewhat too high global temperature, due to a likely interpolation error affecting the two polar regions (see below).*

The Northern Hemisphere was near the average temperature for the previous 10 years, but with pronounced regional differences. Most of Europe and Asia had below average temperatures, while most of North America had above average temperatures. Over the central Arctic region (north of 80°N), however, the interpolated GISS temperature data appears to be affected by an interpolation error, resulting in up to 2-3°C too high temperatures (see lower left diagram on previous page). The resulting anomaly pattern at least looks rather peculiar. Presumably, GISS will correct and remove this feature later.

Near the Equator temperatures were near the 10-year average.

The Southern Hemisphere temperatures were generally near or a little below the previous 10-year average. Australia and central South America had below average temperatures. In the Antarctic, most regions had temperatures above average. However, the central part of the Antarctic (south of 80°S) appears to be affected by the identical error as for the Arctic, although not to the same degree. Most likely, the GISS interpolation here results in up to 1-1.5°C too high temperatures (lower right diagram on previous page).

Temperature quality class 1: Lower troposphere temperature from satellites, updated to November 2016

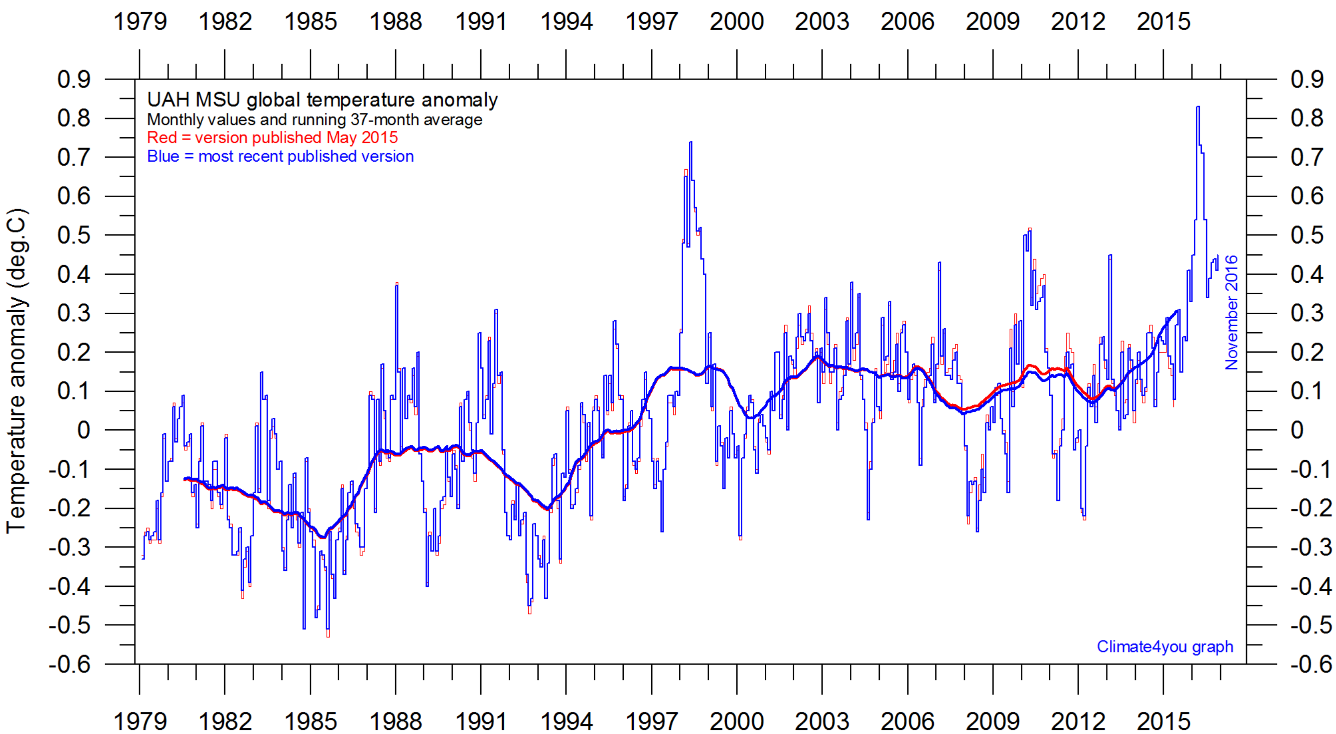

Global monthly average lower troposphere temperature (thin line) since 1979 according to University of Alabama at Huntsville, USA. The thick line is the simple running 37-month average.

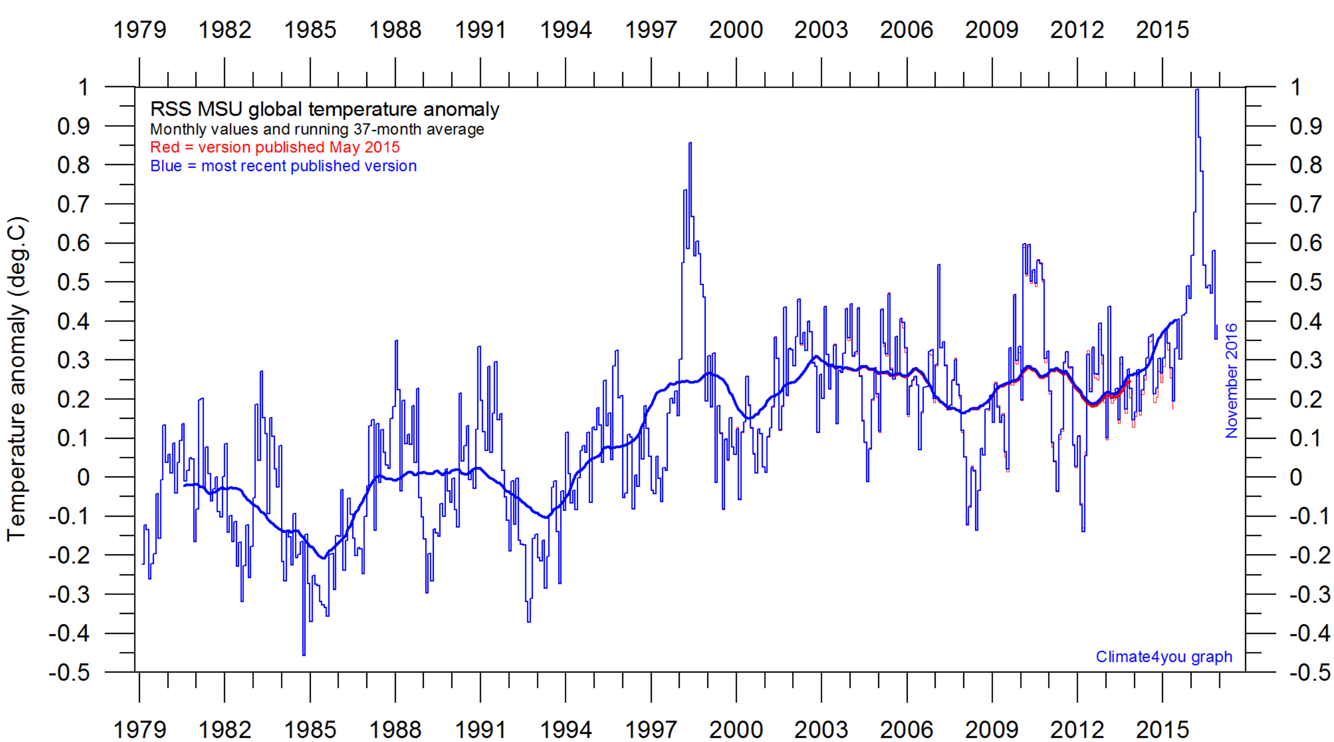

Global monthly average lower troposphere temperature (thin line) since 1979 according to according to Remote Sensing Systems (RSS), USA. The thick line is the simple running 37-month average.

Temperature quality class 2: HadCRUT global surface air temperature, updated to October 2016

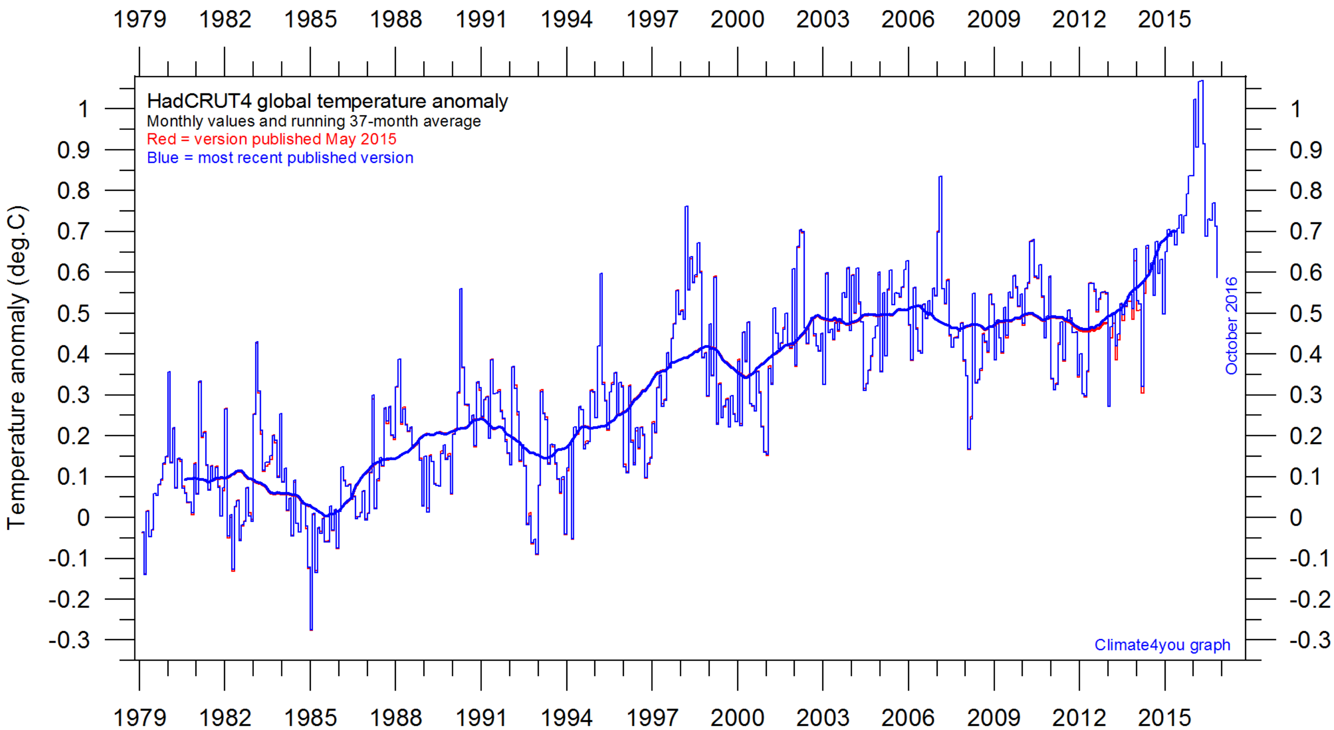

Global monthly average surface air temperature (thin line) since 1979 according to according to the Hadley Centre for Climate Prediction and Research and the University of East Anglia's Climatic Research Unit (CRU), UK. The thick line is the simple running 37-month average. Please note that this diagram is not yet updated beyond October 2016.

Temperature quality class 3: GISS and NCDC global surface air temperature, updated to November 2016

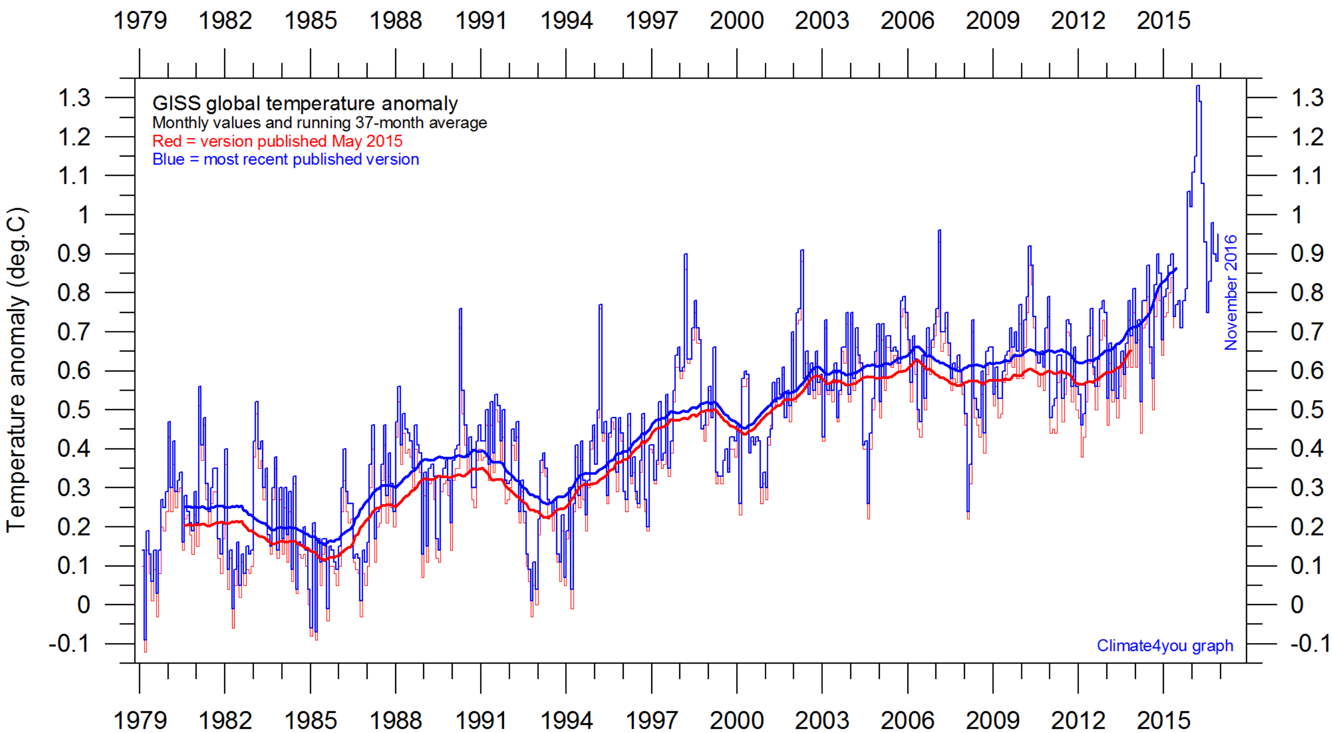

Global monthly average surface air temperature (thin line) since 1979 according to according to the Goddard Institute for Space Studies (GISS), at Columbia University, New York City, USA, using ERSST_v4 ocean surface temperatures. The thick line is the simple running 37-month average.

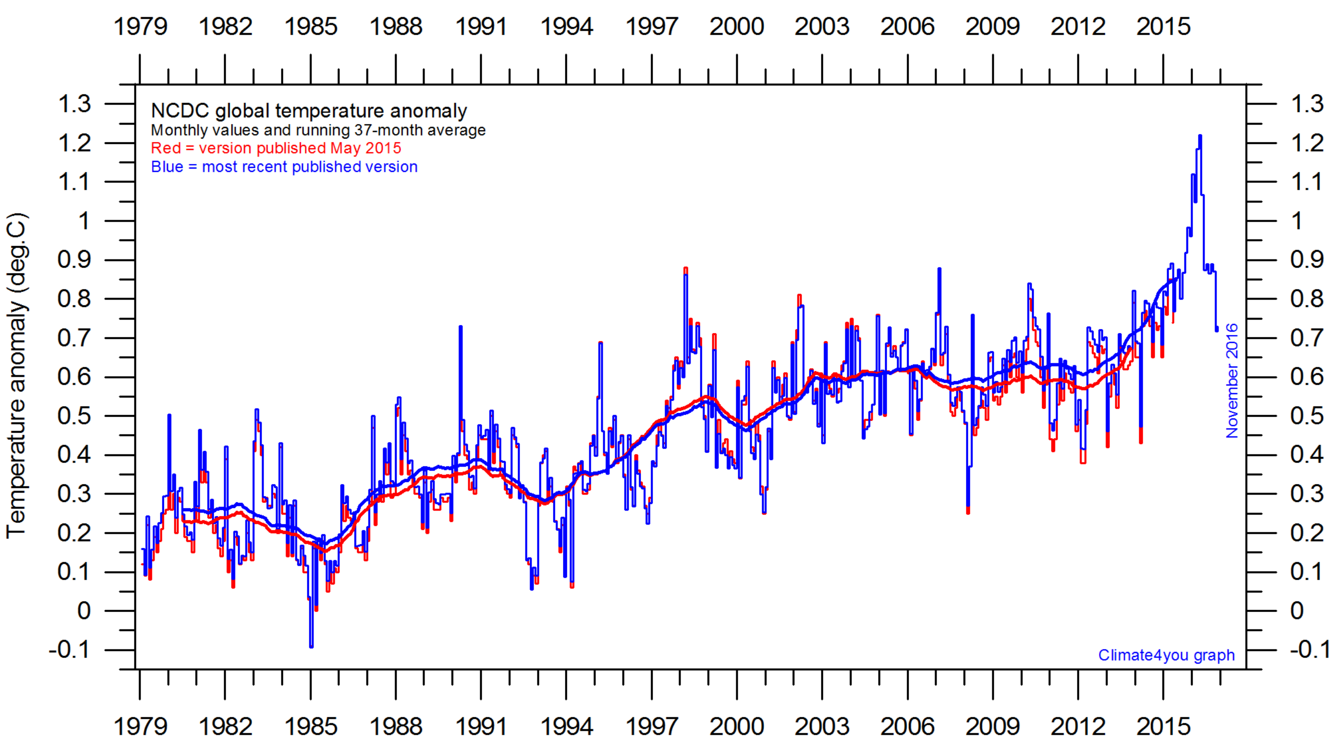

Global monthly average surface air temperature since 1979 according to according to the National Climatic Data Center (NCDC), USA. The thick line is the simple running 37-month average.

A note on data record stability and -quality:

All temperature diagrams shown above have 1979 as starting year. This roughly marks the beginning of the recent period of global warming, after termination of the previous period of global cooling from about 1940. In addition, the year 1979 also represents the starting date for the satellite-based global temperature estimates (UAH and RSS). For the three surface air temperature records (HadCRUT, NCDC and GISS), they begin much earlier (in 1850 and 1880), as can be inspected on www.climate4you.com.

For all three surface air temperature records, but especially NCDC and GISS, administrative changes to anomaly values are quite often introduced, even for observations many years back in time. Some changes may be due to the delayed addition of new station data, while others probably have their origin in a change of technique to calculate average values. It is clearly impossible to evaluate the validity of such administrative changes for the outside user of these records; it is only possible to note that such changes appear very often (se example diagram next page).

In addition, the three surface records represent a blend of sea surface data collected by moving ships or by other means, plus data from land stations of partly unknown quality and unknown degree of representativeness for their region. Many of the land stations have also moved geographically during their existence, and their instrumentation changed, and they are influenced by changes in their surroundings (vegetation, buildings, etc.).

The satellite temperature records also have their problems, but these are generally of a more technical nature and therefore correctable. In addition, the temperature sampling by satellites is more regular and complete on a global basis than that represented by the surface records. Also important is that the sensors on satellites measure temperature directly by emitted radiation, while most surface temperature measurements are indirect, using electronic resistance.

Everybody interested in climate science should gratefully acknowledge the efforts put into maintaining the different temperature databases referred to in the present newsletter. At the same time, however, it is also important to realise that all temperature records cannot be of equal scientific quality. The simple fact that they to some degree differ shows that they cannot all be correct.

On this background, and for practical reasons, Climate4you operates with three quality classes (1-3) for global temperature records, with 1 representing the highest quality level:

Quality class 1: The satellite records (UAH and RSS).

Quality class 2: The HadCRUT surface record.

Quality class 3: The NCDC and GISS surface records.

The main reason for discriminating between the three surface records is the following:

While both NCDC and GISS often experience quite large administrative changes (see example on p.8), and therefore essentially are unstable temperature records, the changes introduced to HadCRUT are fewer and smaller. For obvious reasons, as the past does not change, any record undergoing continuing changes cannot describe the past correctly all the time.

You can find more on the issue of lack of temporal stability on www.climate4you.com (go to: *Global Temperature*, followed by *Temporal Stability*).

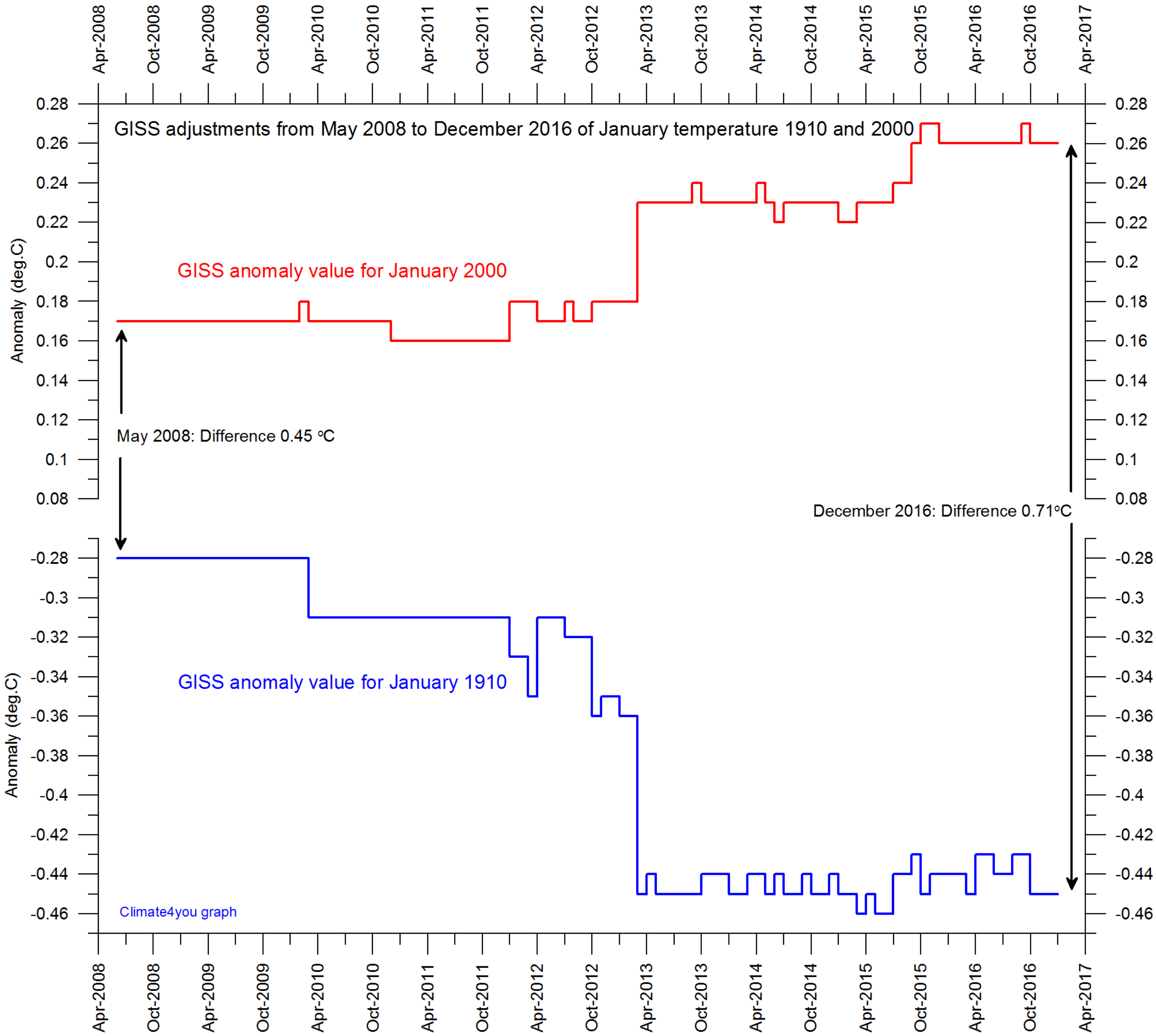

Diagram showing the adjustment made since May 2008 by the Goddard Institute for Space Studies (GISS), USA, in anomaly values for the months January 1910 and January 2000.

Note: The administrative upsurge of the temperature increase from January 1915 to January 2000 has grown from 0.45 (reported May 2008) to 0.71°C (reported December 2016). This represents an about 58% administrative temperature increase over this period, meaning that more than half of the reported (by GISS) global temperature increase from January 1910 to January 2000 is due to administrative changes of the original data since May 2008.

Comparing global surface air temperature and lower troposphere satellite temperatures; updated to October 2016

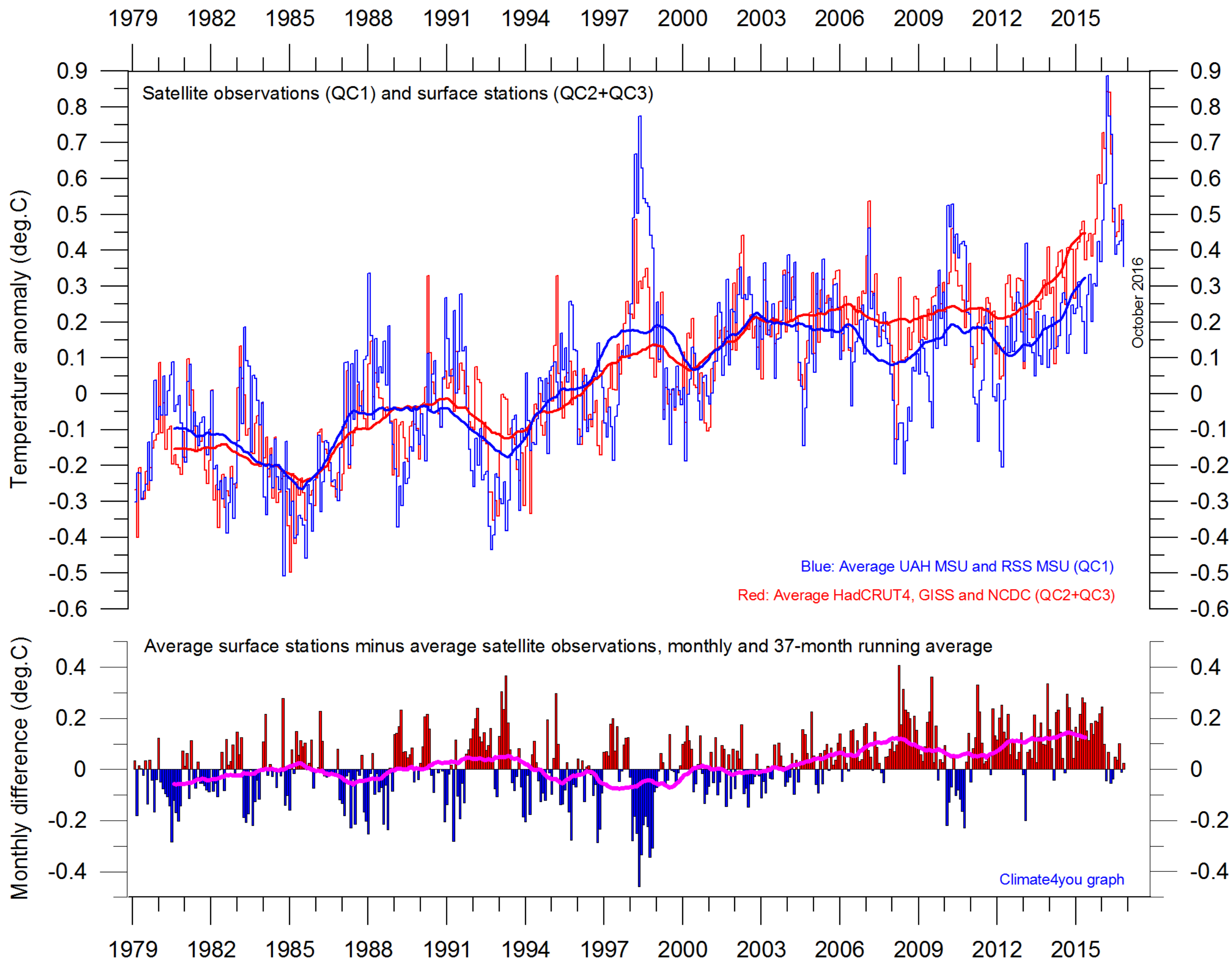

Plot showing the average of monthly global surface air temperature estimates (HadCRUT4, GISS and NCDC) and satellite-based temperature estimates (RSS MSU and UAH MSU). The thin lines indicate the monthly value, while the thick lines represent the simple running 37 month average, nearly corresponding to a running 3 yr average. The lower panel shows the monthly difference between average surface air temperature and satellite temperatures. As the base period differs for the different temperature estimates, they have all been normalised by comparing to the average value of 30 years from January 1979 to December 2008.

NOTE: Since about 2003, the average global surface air temperature is steadily drifting away in positive direction from the average satellite temperature, meaning that the surface records show warming in relation to the troposphere records. The reason(s) for this is not entirely clear, but can presumably at least partly be explained by the recurrent administrative adjustments made to the surface records (see p. 7-8).

Global air temperature linear trends updated to October 2016

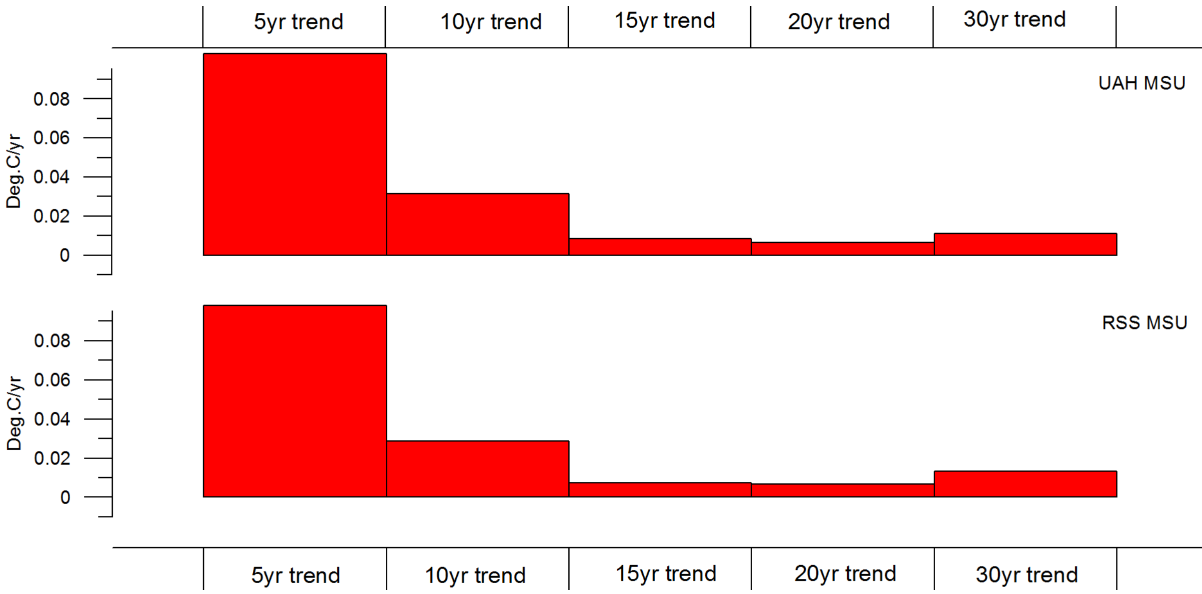

Diagram showing the latest 5, 10, 20 and 30 yr linear annual global temperature trend, calculated as the slope of the linear regression line through the data points, for two satellite-based temperature estimates (UAH MSU and RSS MSU).

Diagram showing the latest 5, 10, 20, 30, 50, 70 and 100 year linear annual global temperature trend, calculated as the slope of the linear regression line through the data points, for three surface-based temperature estimates (GISS, NCDC and HadCRUT4).

All in one, Quality Class 1, 2 and 3; updated to November 2016

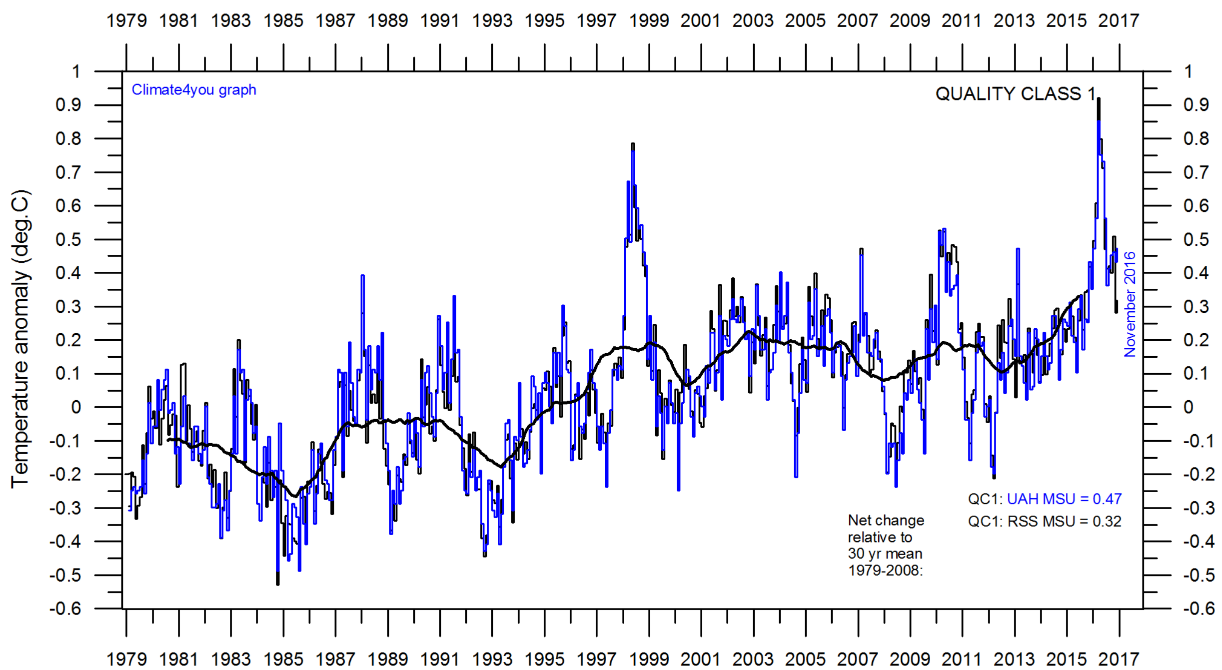

Superimposed plot of Quality Class 1 (UAH and RSS) global monthly temperature estimates. As the base period differs for the individual temperature estimates, they have all been normalised by comparing with the average value of the initial 120 months (30 years) from January 1979 to December 2008. The heavy black line represents the simple running 37 month (c. 3 year) mean of the average of both temperature records. The numbers shown in the lower right corner represent the temperature anomaly relative to the individual 1979-2008 averages.

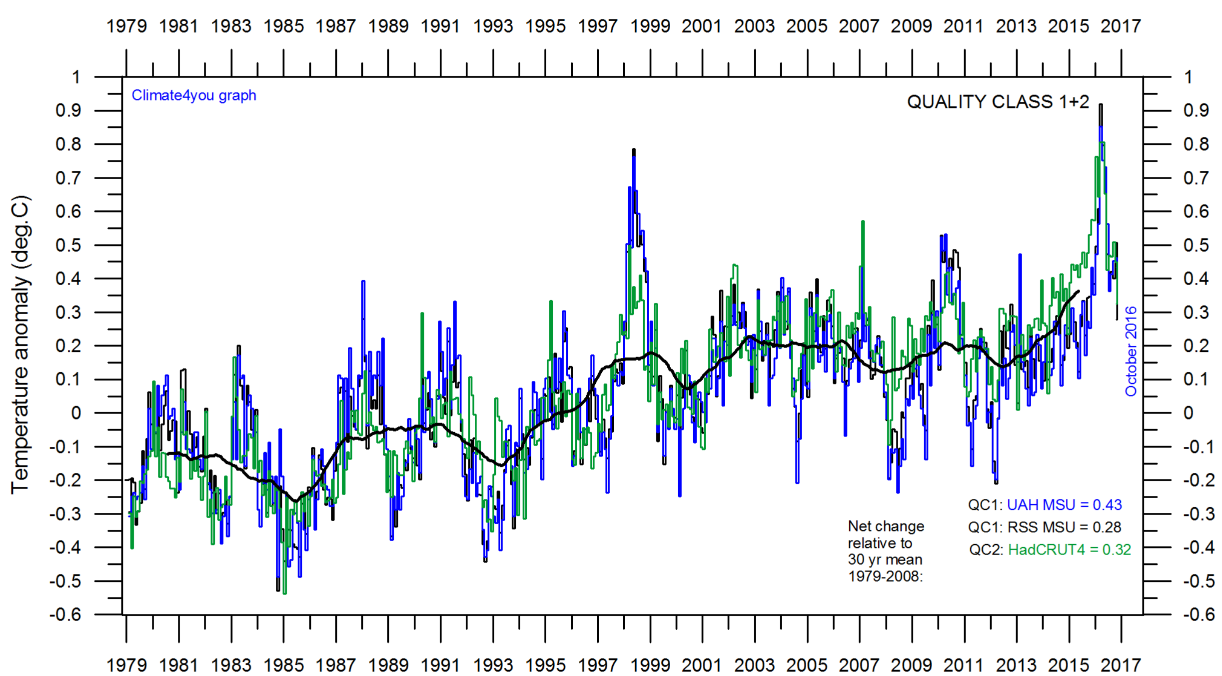

Superimposed plot of Quality Class 1 and 2 (UAH, RSS and HadCRUT4) global monthly temperature estimates. As the base period differs for the individual temperature estimates, they have all been normalised by comparing with the average value of the initial 120 months (30 years) from January 1979 to December 2008. The heavy black line represents the simple running 37 month (c. 3 year) mean of the average of all three temperature records. The numbers shown in the lower right corner represent the temperature anomaly relative to the individual 1979-2008 averages.

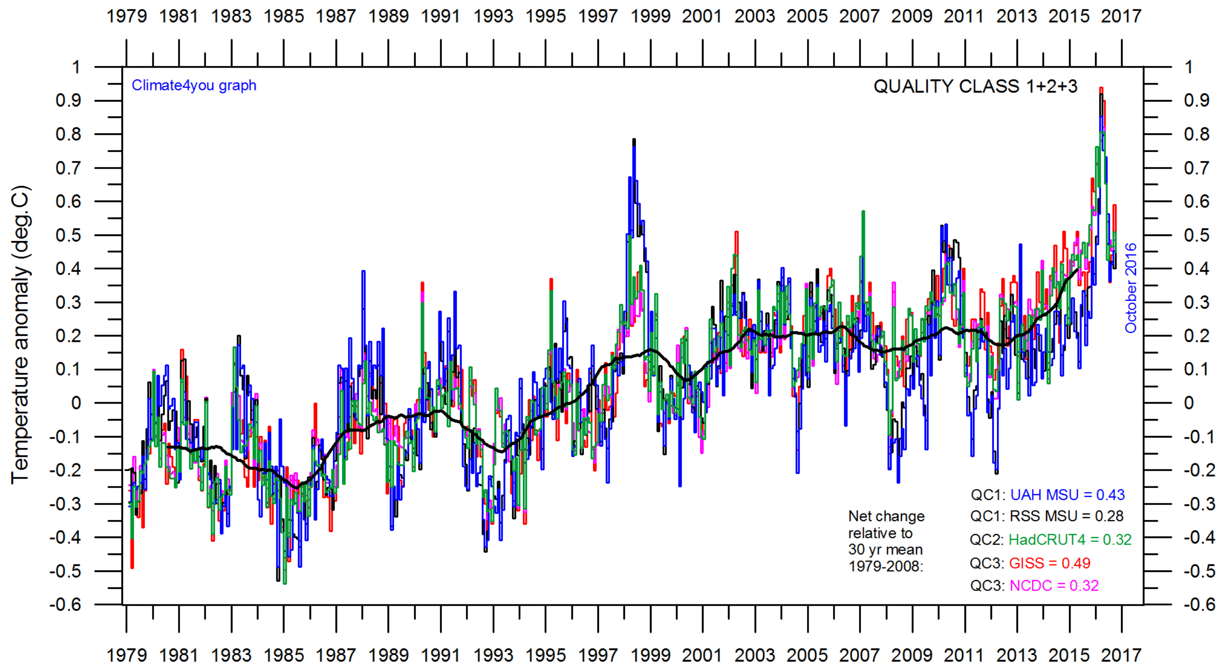

Superimposed plot of Quality Class 1, 2 and 3 global monthly temperature estimates (UAH, RSS, HadCRUT4, GISS and NCDC). As the base period differs for the individual temperature estimates, they have all been normalised by comparing with the average value of the initial 120 months (30 years) from January 1979 to December 2008. The heavy black line represents the simple running 37 month (c. 3 year) mean of the average of all five temperature records. The numbers shown in the lower right corner represent the temperature anomaly relative to the individual 1979-2008 averages.

Please see notes on page 7 relating to the above three quality classes.

It should be kept in mind that satellite- and surface-based temperature estimates are derived from different types of measurements, and that comparing them directly as done in the diagram above therefore may be somewhat problematical. However, as both types of estimate often are discussed together, the above diagram may nevertheless be of some interest. In fact, the different types of temperature estimates appear to agree as to the overall temperature variations on a 2-3 year scale, although on a shorter time scale there are often considerable differences between the individual records. However, since about 2003 the surface records are consistently drifting towards higher temperatures than the satellite records (see p. 9).

The average of all five global temperature estimates presently shows an overall stagnation, at least since 2002-2003. There has been no real increase in global air temperature since 1998, which however was affected by the oceanographic El Niño event. Also, the recent (2015-16) El Niño event is probably a relatively short-lived spike on a longer development. Neither has there been a temperature decrease since 2002-2003.

The present temperature stagnation does not exclude the possibility that global temperatures will begin to increase again later. On the other hand, it also remains a possibility that Earth just now is passing a temperature peak, and that global temperatures will begin to decrease during the coming years. Time will show which of these two possibilities is correct.

Global sea surface temperature, updated to November 2016

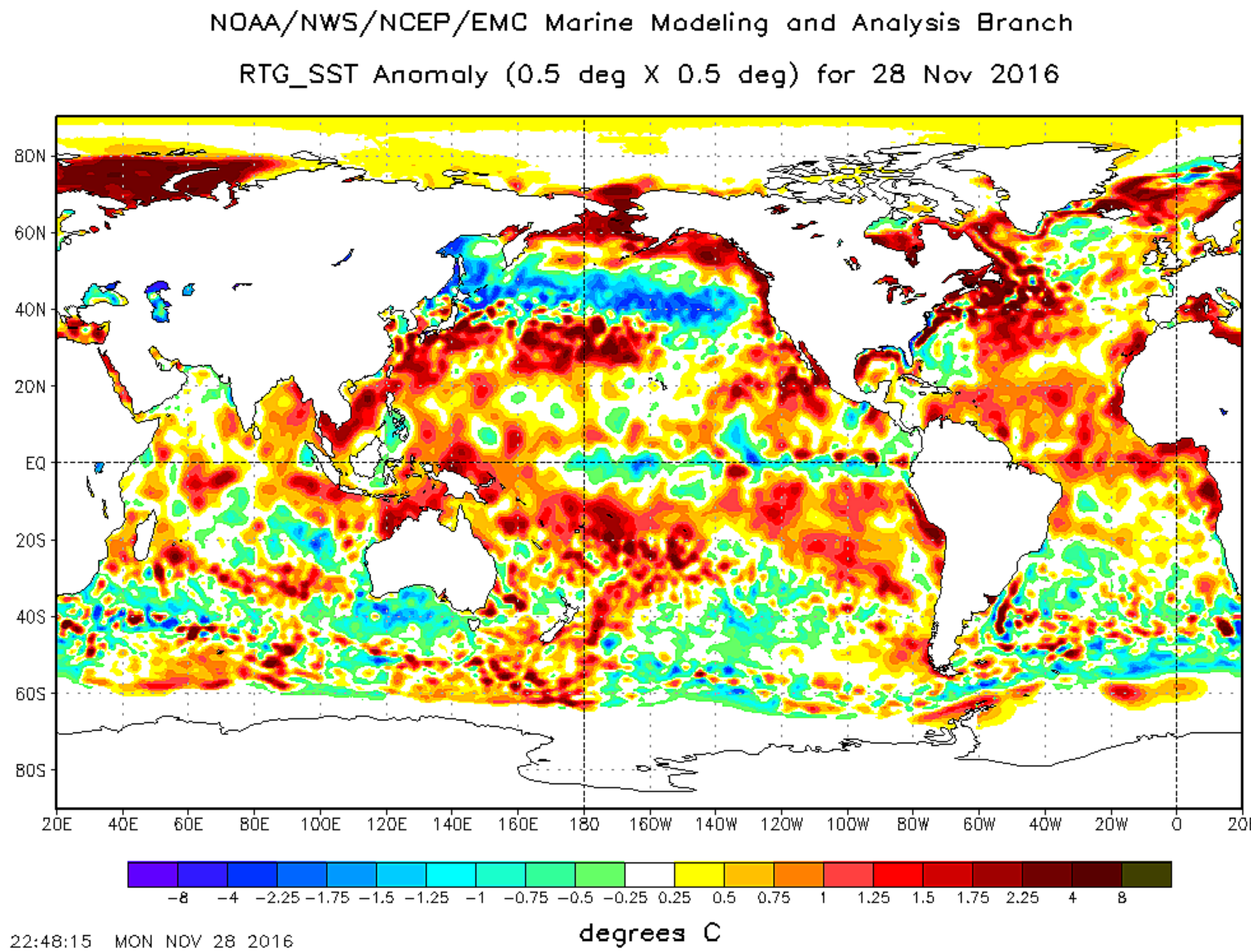

Sea surface temperature anomaly on 28 November 2016. Map source: National Centers for Environmental Prediction (NOAA).

Because of the large surface areas near Equator, the temperature of the surface water in these regions is especially important for the global atmospheric temperature (p.4-6).

Relatively warm water is still dominating much of the oceans near the Equator, and is influencing global air temperatures now and in the months to come.

The significance of any short-term cooling or warming reflected in air temperatures should not be overstated. Whenever Earth experiences cold La Niña or warm El Niño episodes (Pacific Ocean) major heat exchanges takes place between the Pacific Ocean and the atmosphere above, eventually showing up in estimates of the global air temperature.

However, this does not reflect similar changes in the total heat content of the atmosphere-ocean system. In fact, global net changes can be small and such heat exchanges may mainly reflect redistribution of energy between ocean and atmosphere. What matters is the overall temperature development when seen over a number of years.

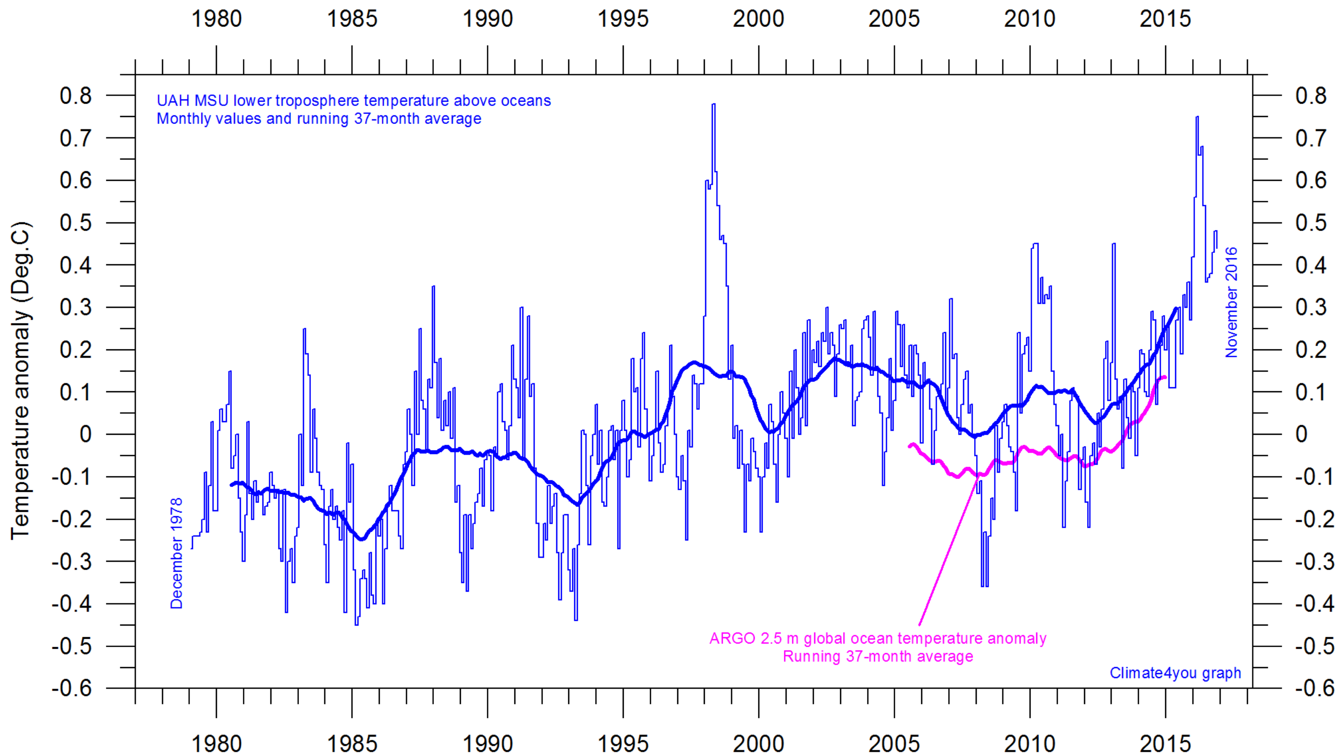

Global monthly average lower troposphere temperature over oceans (thin line) since 1979 according to [University of Alabama](#) at Huntsville, USA. The thick line is the simple running 37 month average. Insert: Argo global ocean temperature anomaly from floats.

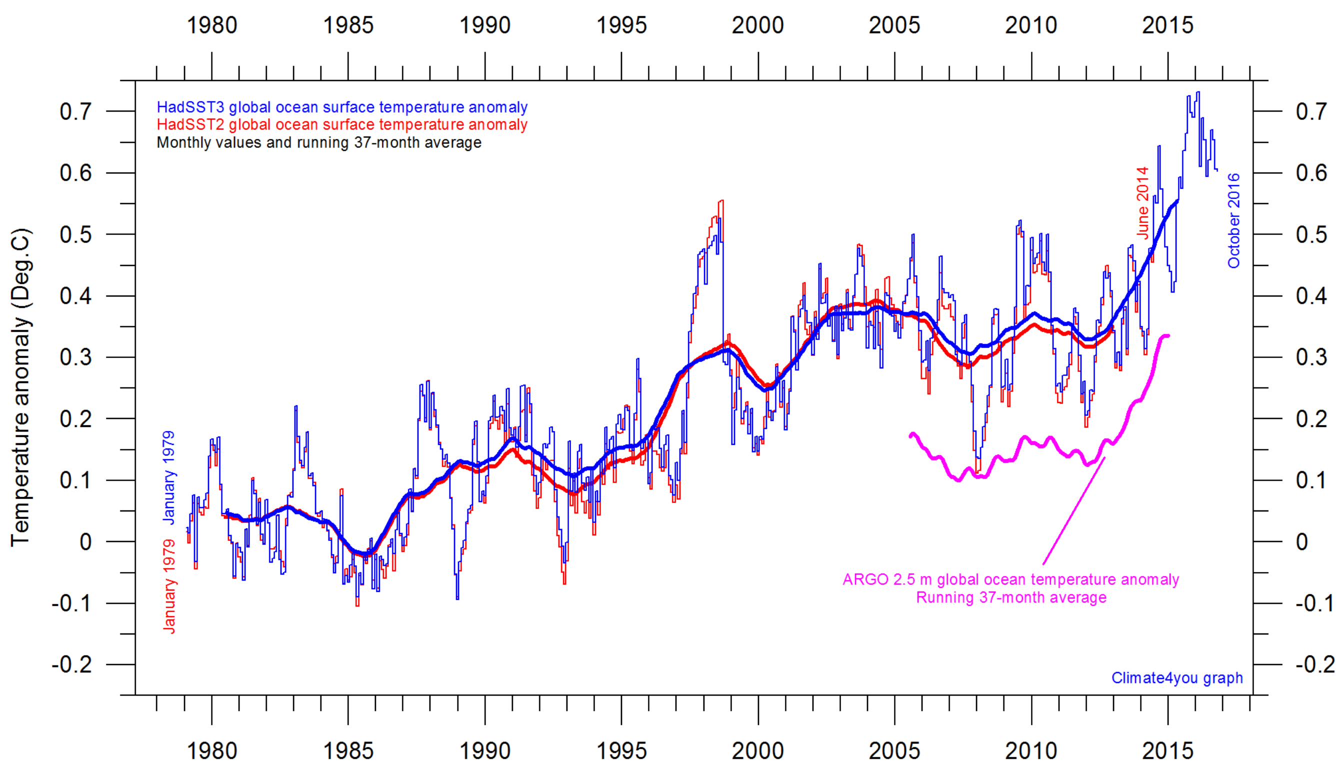

Global monthly average sea surface temperature since 1979 according to University of East Anglia's [Climatic Research Unit](#) ([CRU](#)), UK. Base period: 1961-1990. The thick line is the simple running 37-month average. Insert: Argo global ocean temperature anomaly from floats. Please note that this diagram has not yet been updated beyond October 2016.

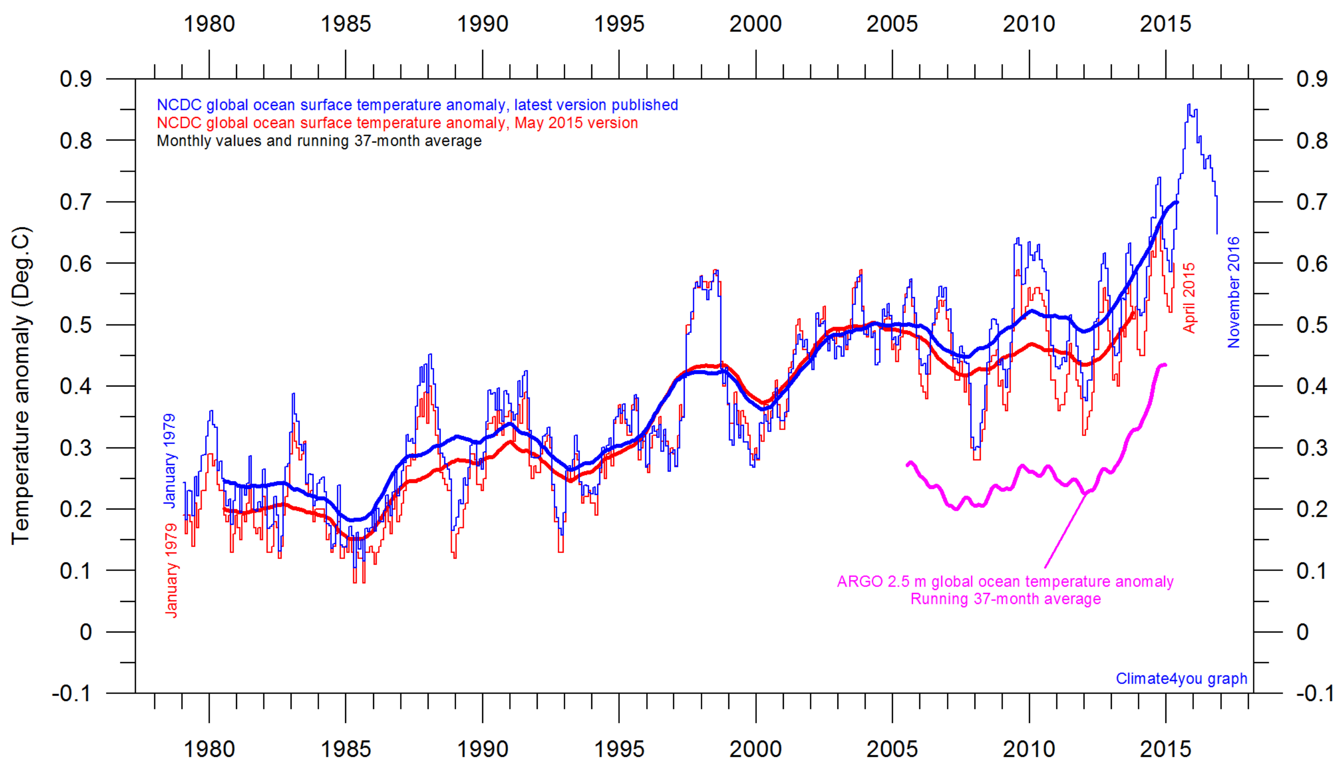

Global monthly average sea surface temperature since 1979 according to the National Climatic Data Center (NCDC), USA. Base period: 1901-2000. The thick line is the simple running 37-month average. Insert: Argo global ocean temperature anomaly from floats.

June 18, 2015: *NCDC has introduced a number of rather large administrative changes to their sea surface temperature record. The overall result is to produce a record giving the impression of a continuous temperature increase, also in the 21st century. As the oceans cover about 71% of the entire surface of planet Earth, the effect of this administrative change is clearly seen in the NCDC record for global surface air temperature (p. 6).*

Ocean temperature in uppermost 100 m, updated to September 2016

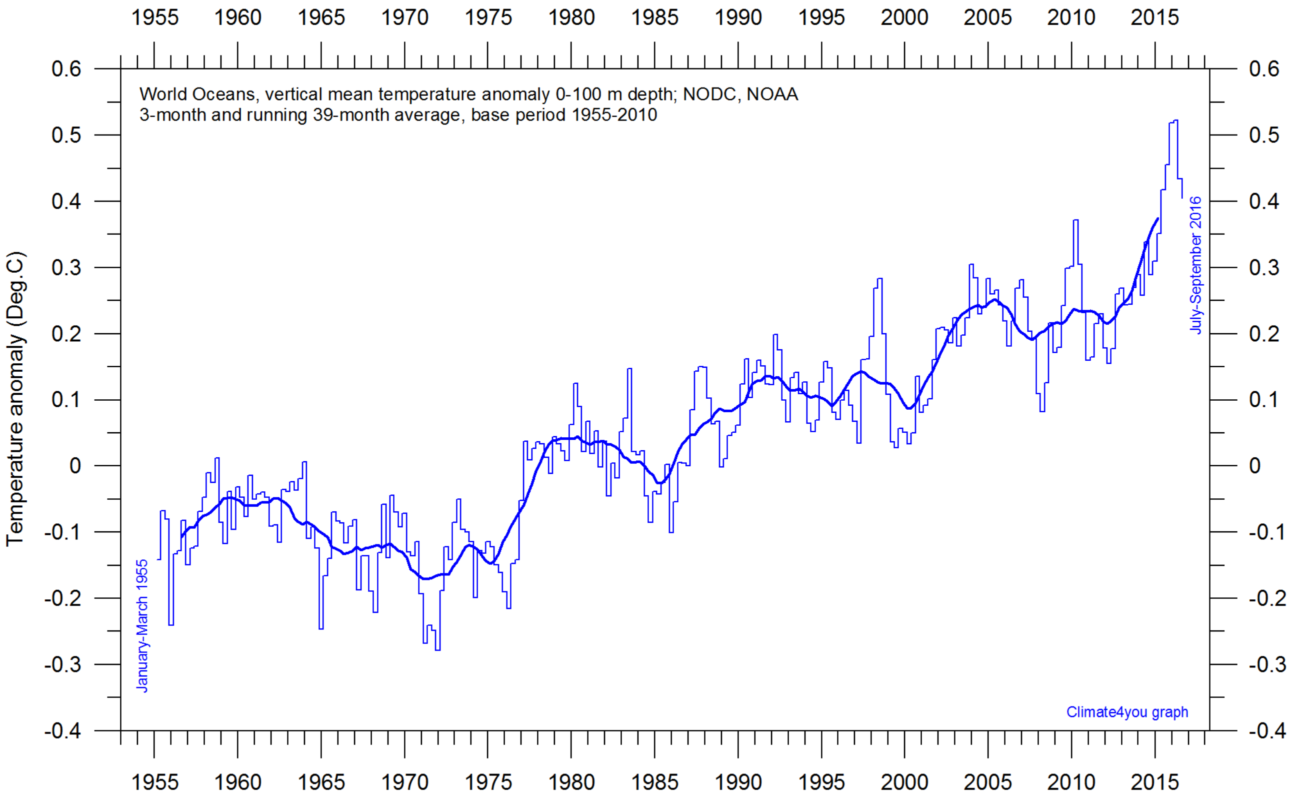

World Oceans vertical average temperature 0-100 m depth since 1955. The thin line indicates 3-month values, and the thick line represents the simple running 39-month (c. 3 year) average. Data source: NOAA National Oceanographic Data Center (NODC). Base period 1955-2010.

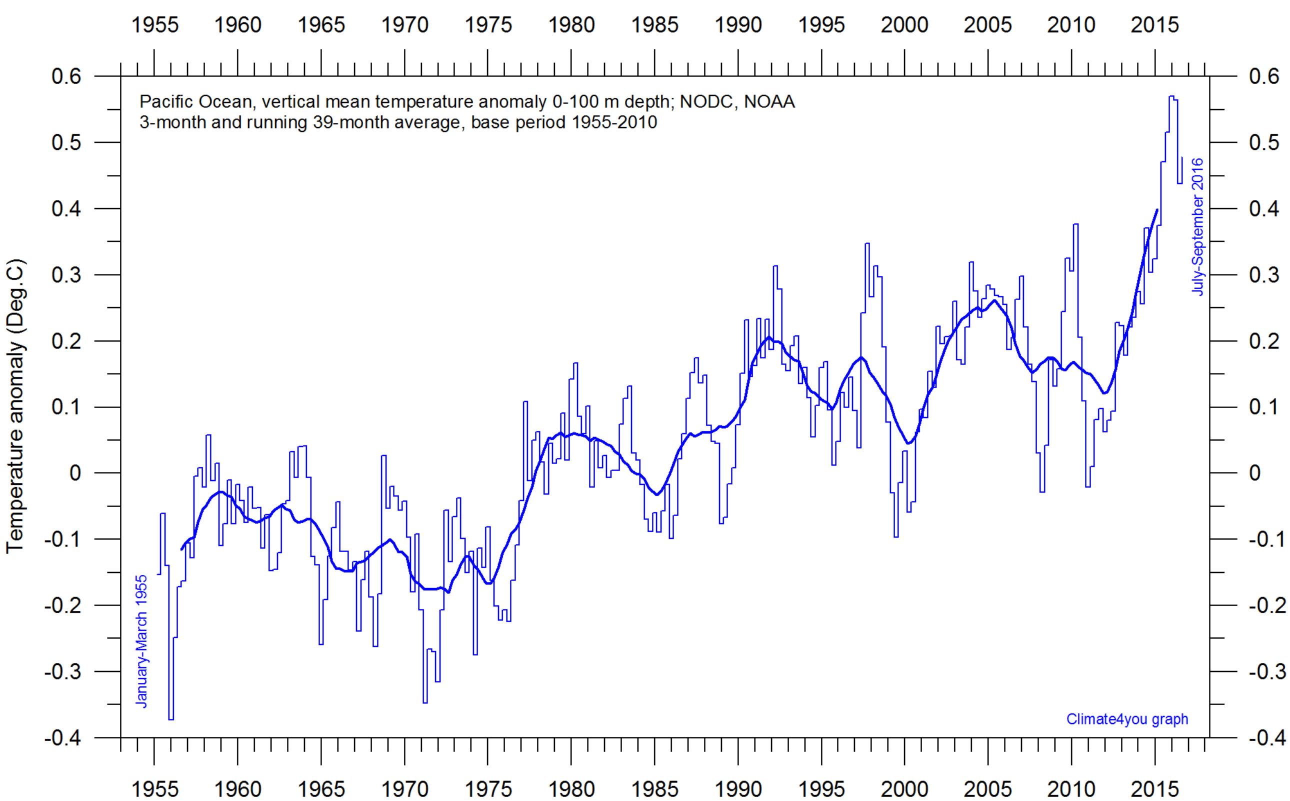

Pacific Ocean vertical average temperature 0-100 m depth since 1955. The thin line indicate 3-month values, and the thick line represents the simple running 39-month (c. 3 year) average. Data source: NOAA National Oceanographic Data Center (NODC). Base period 1955-2010.

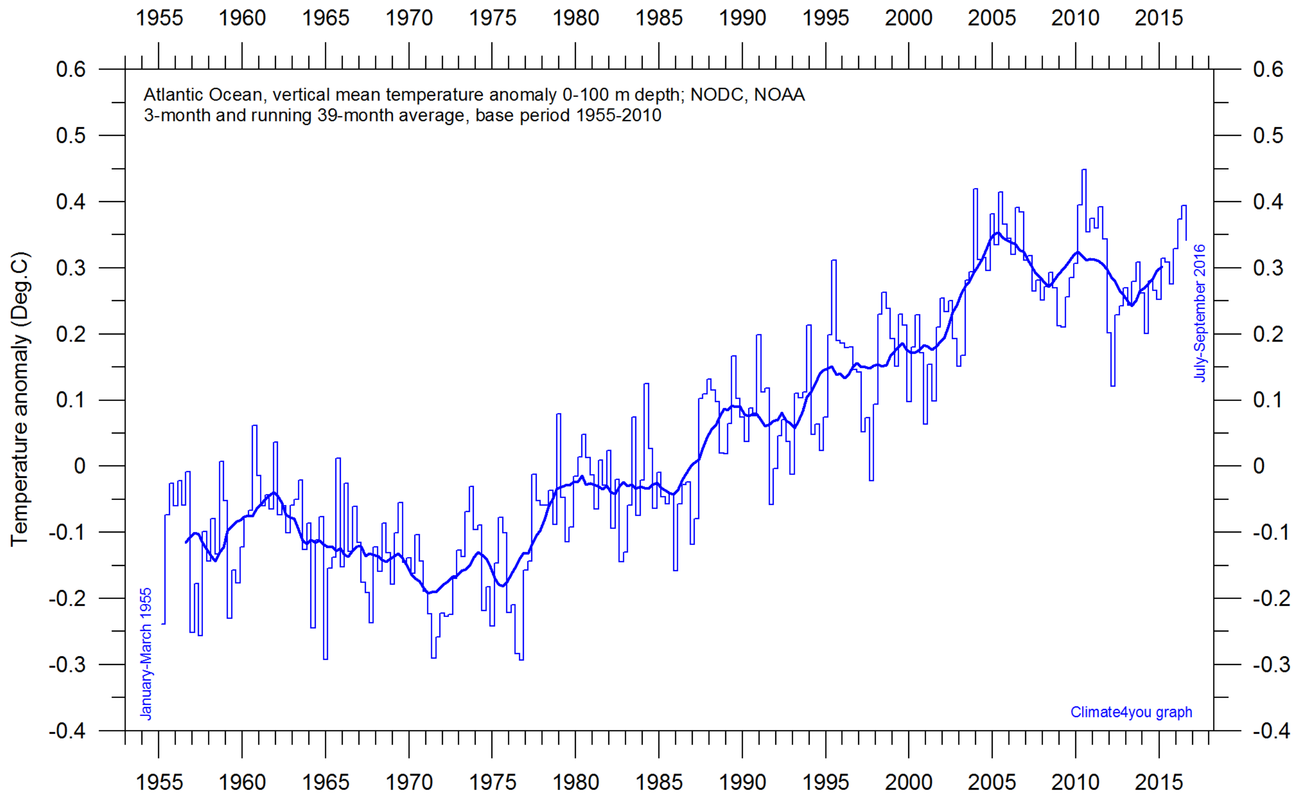

Atlantic Ocean vertical average temperature 0-100 m depth since 1955. The thin line indicate 3-month values, and the thick line represents the simple running 39-month (c. 3 year) average. Data source: NOAA National Oceanographic Data Center (NODC). Base period 1955-2010.

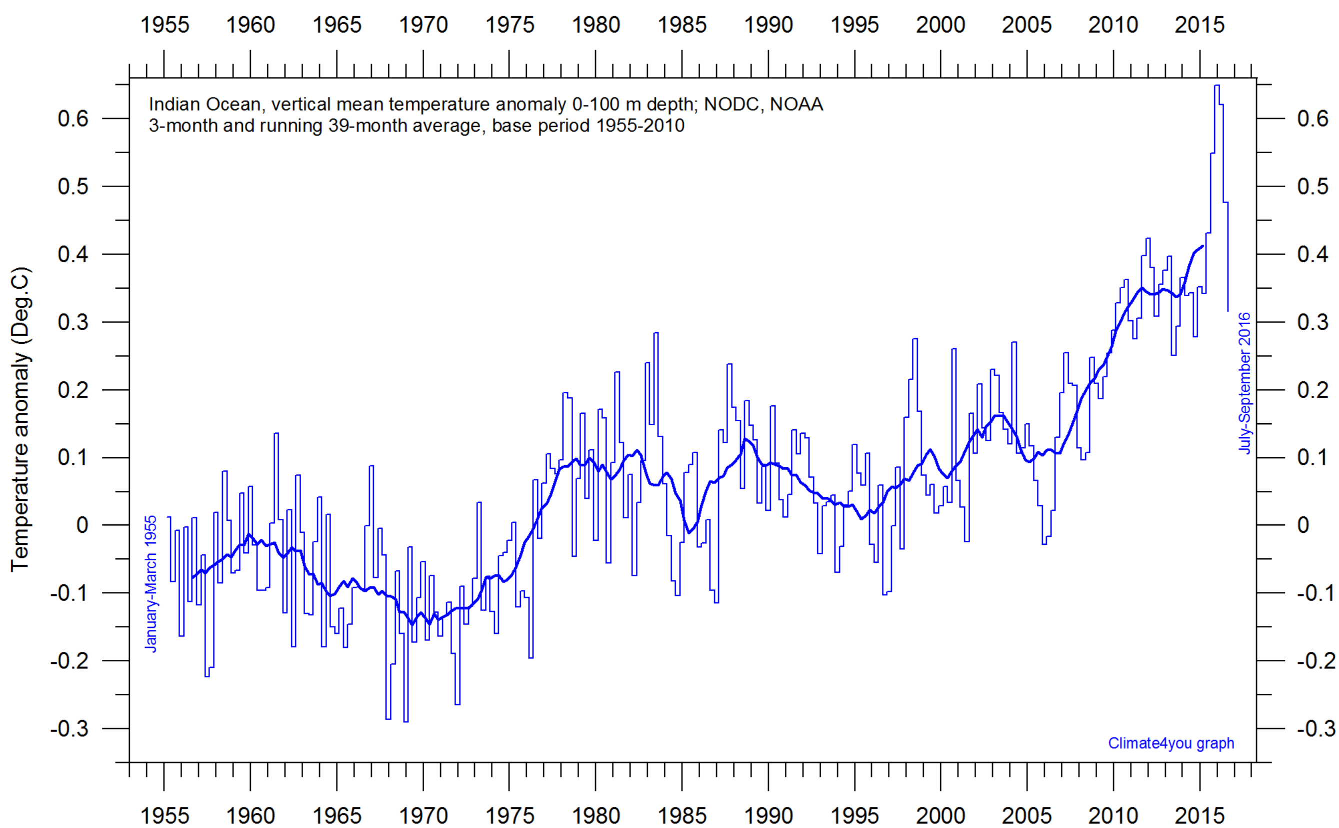

Indian Ocean vertical average temperature 0-100 m depth since 1955. The thin line indicate 3-month values, and the thick line represents the simple running 39-month (c. 3 year) average. Data source: NOAA National Oceanographic Data Center (NODC). Base period 1955-2010.

North Atlantic heat content uppermost 700 m, updated to September 2016

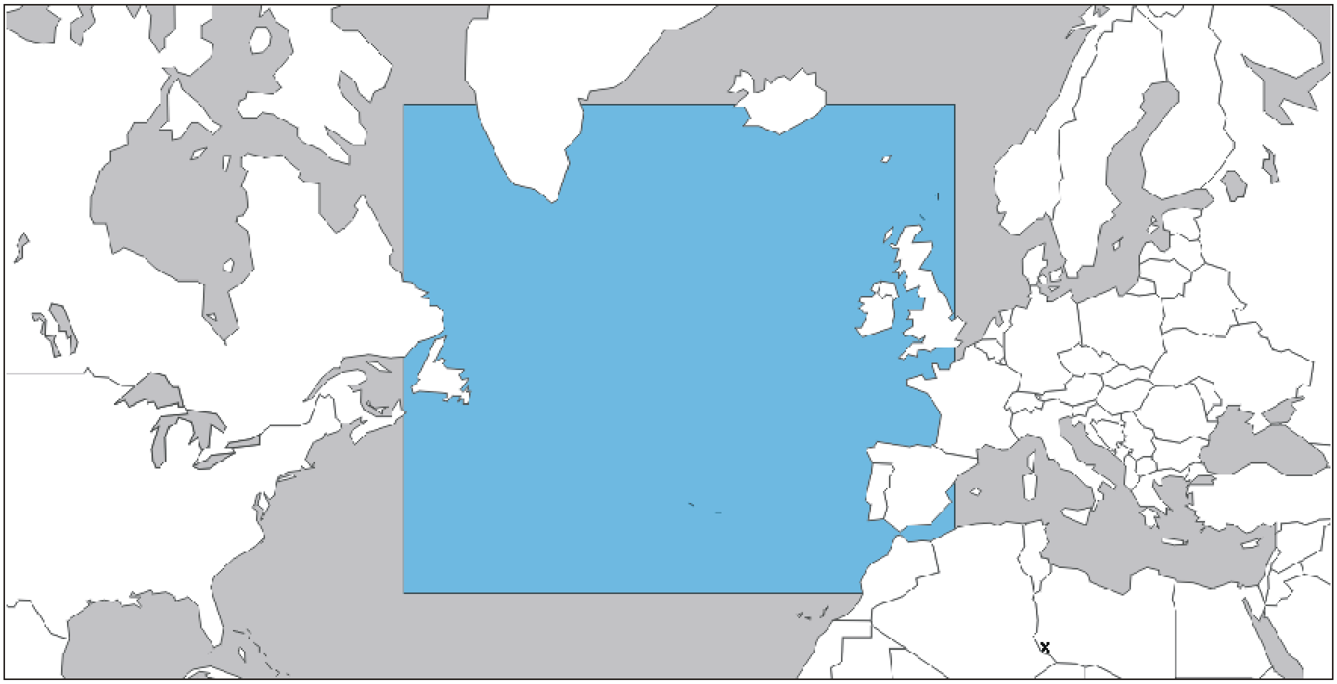

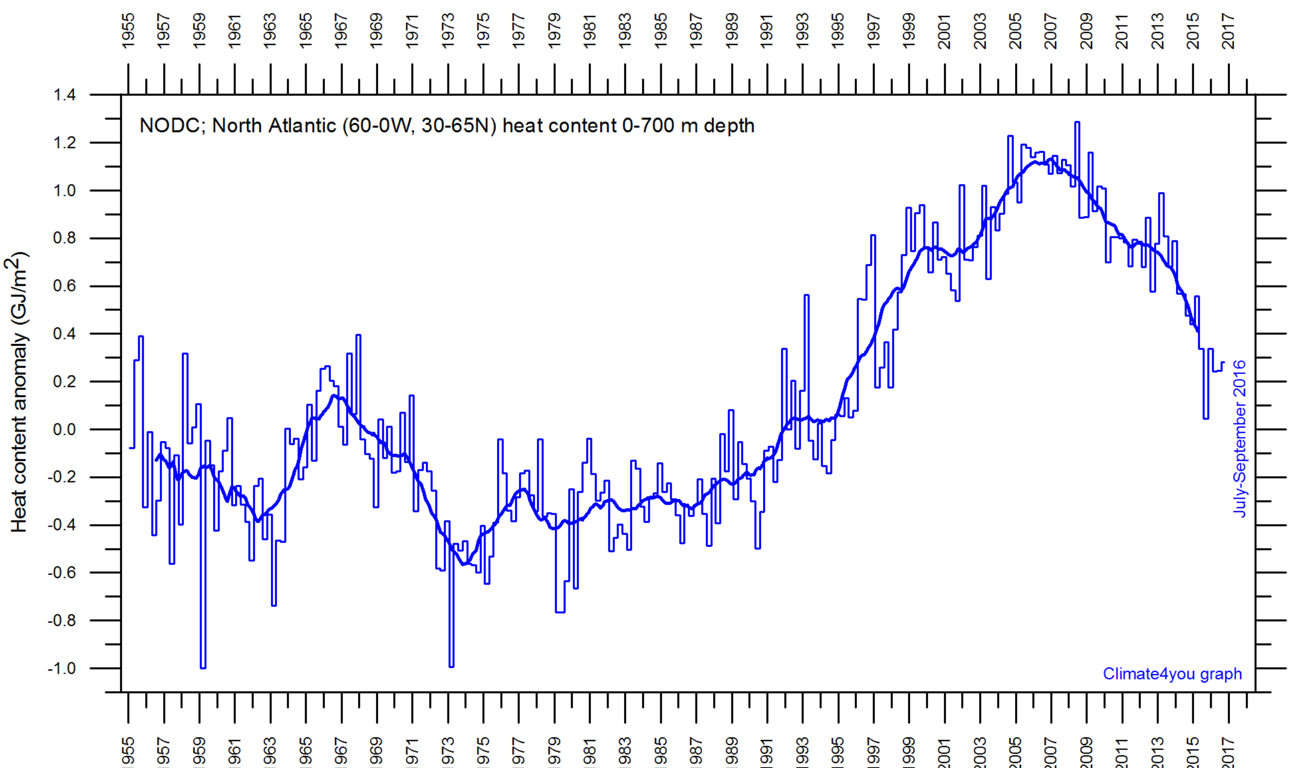

Global monthly heat content anomaly (GJ/m2) in the uppermost 700 m of the North Atlantic (60-0W, 30-65N; see map above) *ocean since January 1955. The thin line indicates monthly values, and the thick line represents the simple running 37 month (c. 3 year) average. Data source: National Oceanographic Data Center (NODC).*

19

North Atlantic temperatures 0-800 m depth along 59°N, 30-0W, updated to June 2016

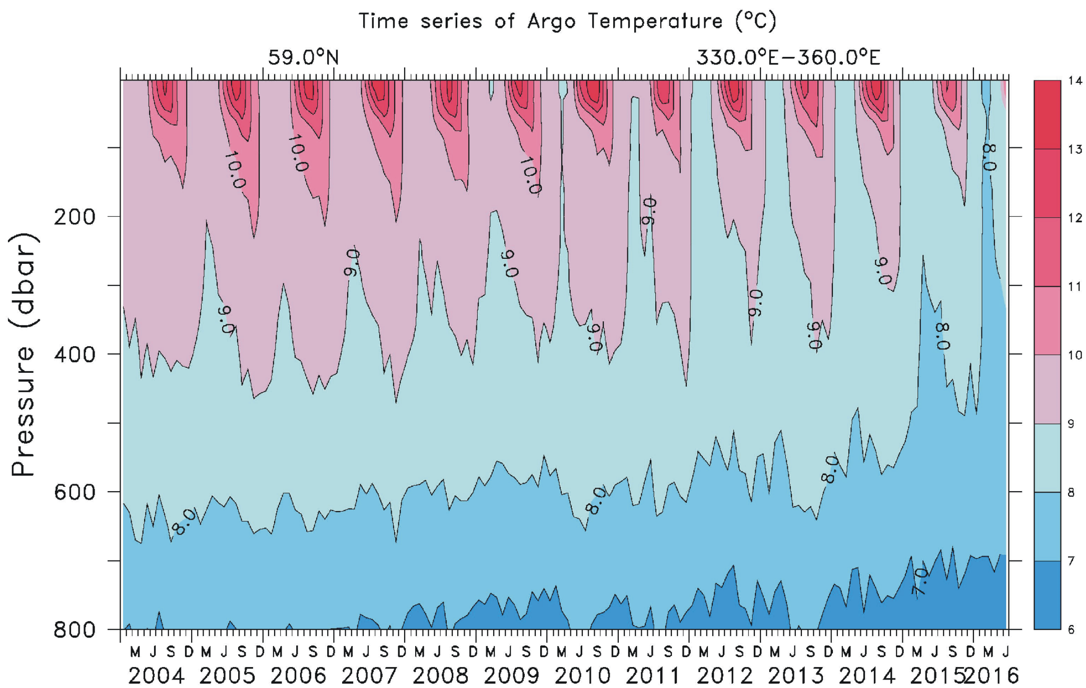

Time series depth-temperature diagram along 59 N across the North Atlantic Current from 30°W to 0°W, from surface to 800 m depth. Source: Global Marine Argo Atlas. See also the diagram below.

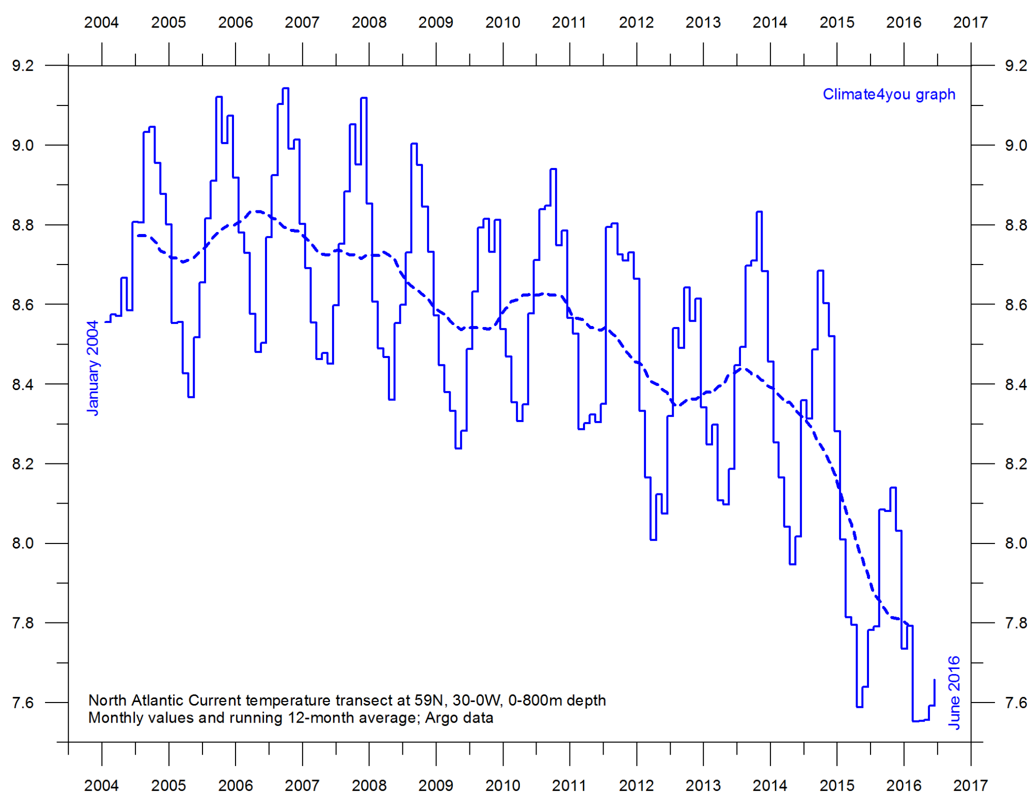

Average temperature along 59 N, 30-0W, 0-800m depth, corresponding to the main part of the North Atlantic Current, using Argo-data. Source: Global Marine Argo Atlas. Additional information can be found in: Roemmich, D. and J. Gilson, 2009. The 2004-2008 mean and annual cycle of temperature, salinity, and steric height in the global ocean from the Argo Program. Progress in Oceanography, 82, 81-100.

Global ocean temperature 0-2000 m depth summary, updated to June 2016

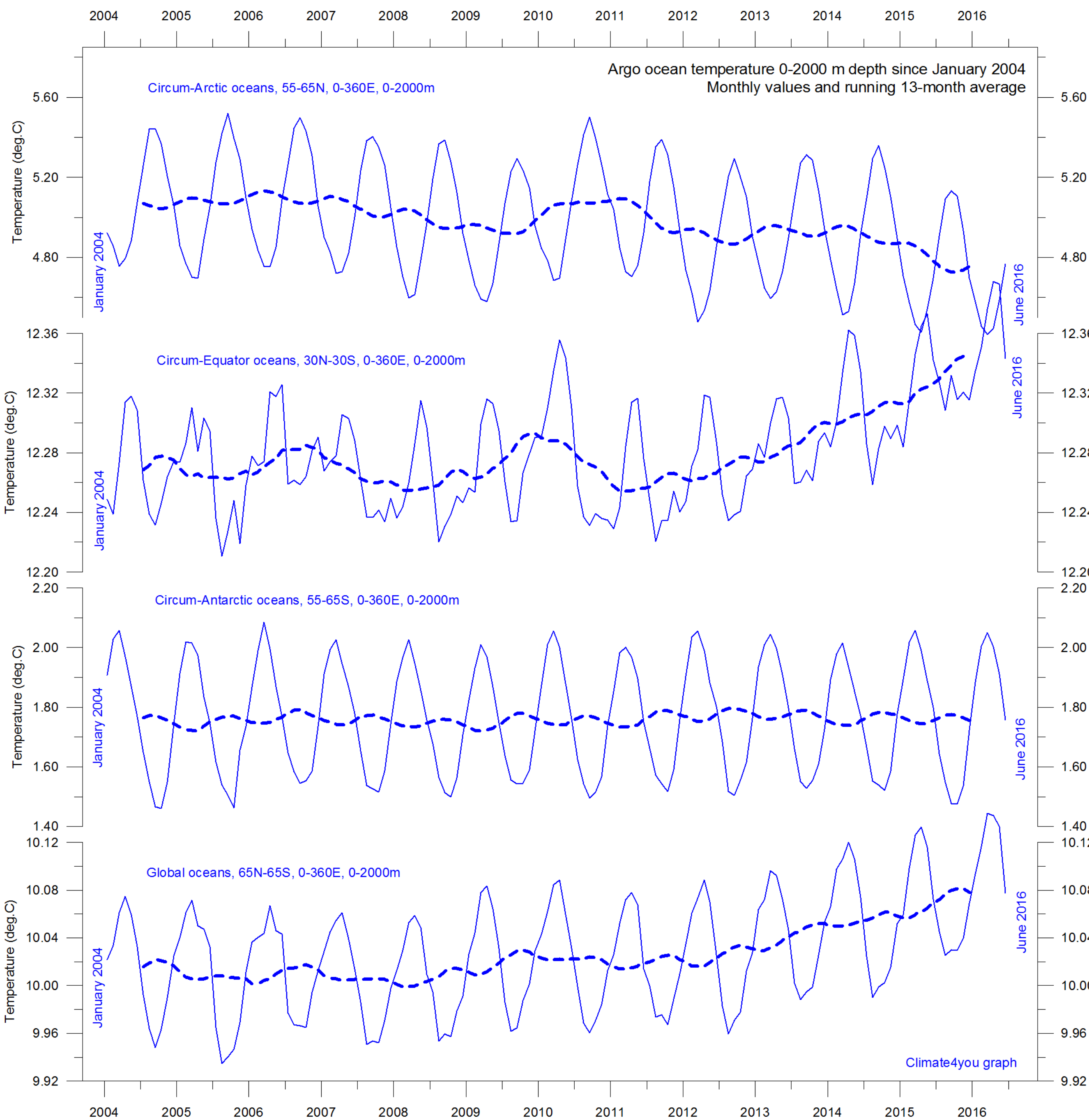

Summary of average temperature in uppermost 2000 m in different parts of the global oceans, using Argo-data. Source: Global Marine Argo Atlas. Additional information can be found in: Roemmich, D. and J. Gilson, 2009. The 2004-2008 mean and annual cycle of temperature, salinity, and steric height in the global ocean from the Argo Program. Progress in Oceanography, 82, 81-100.

Troposphere and stratosphere temperatures from satellites, updated to November 2016

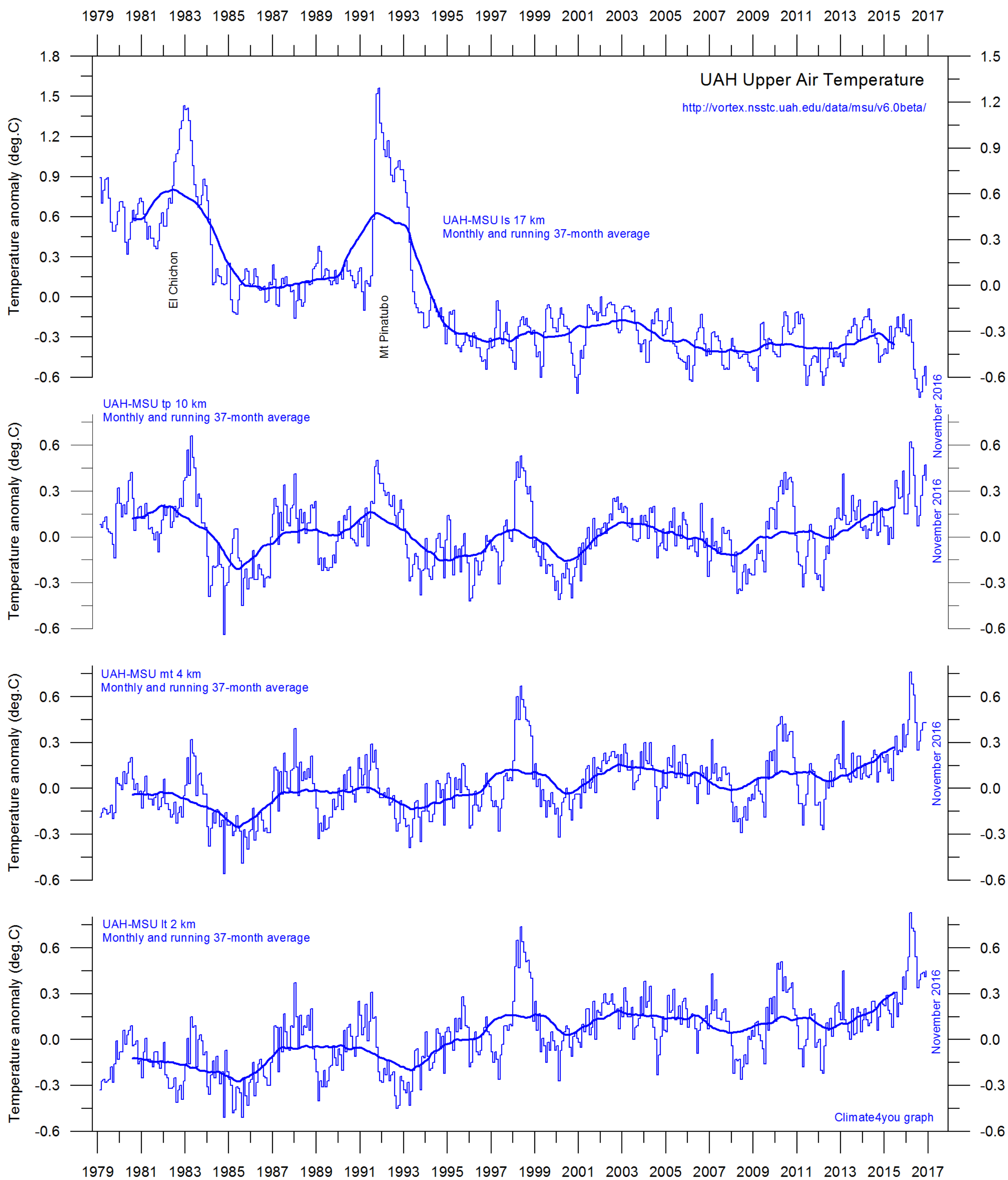

Global monthly average temperature in different according to University of Alabama at Huntsville, USA. The thin lines represent the monthly average, and the thick line the simple running 37 month average, nearly corresponding to a running 3 year average.

Zonal lower troposphere temperatures from satellites, updated to November 2016

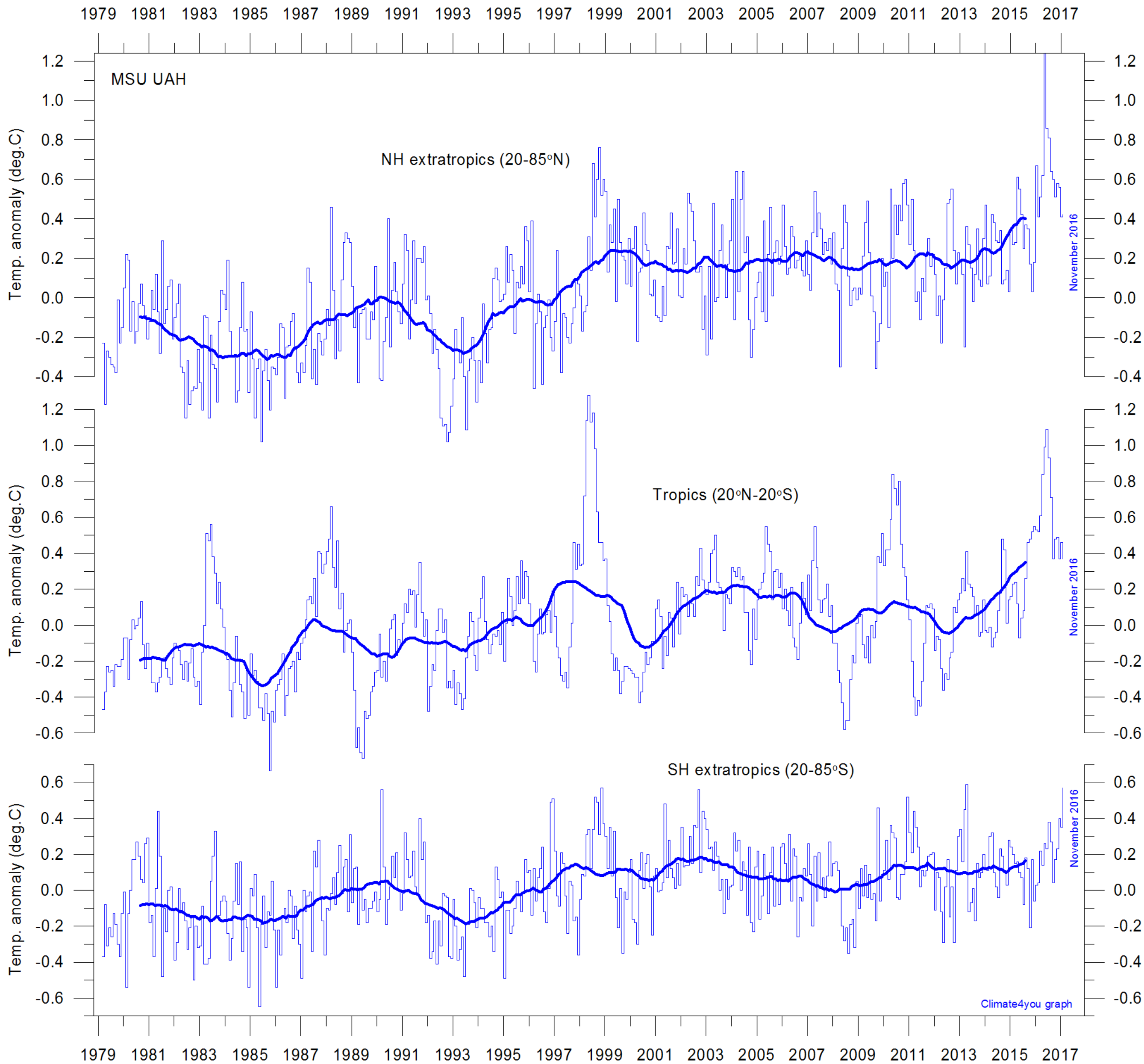

Global monthly average lower troposphere temperature since 1979 for the tropics and the northern and southern extratropics, according to University of Alabama at Huntsville, USA. Thin lines show the monthly temperature. Thick lines represent the simple running 37-month average, nearly corresponding to a running 3 year average. Reference period 1981-2010.

Arctic and Antarctic lower troposphere temperature, updated to November 2016

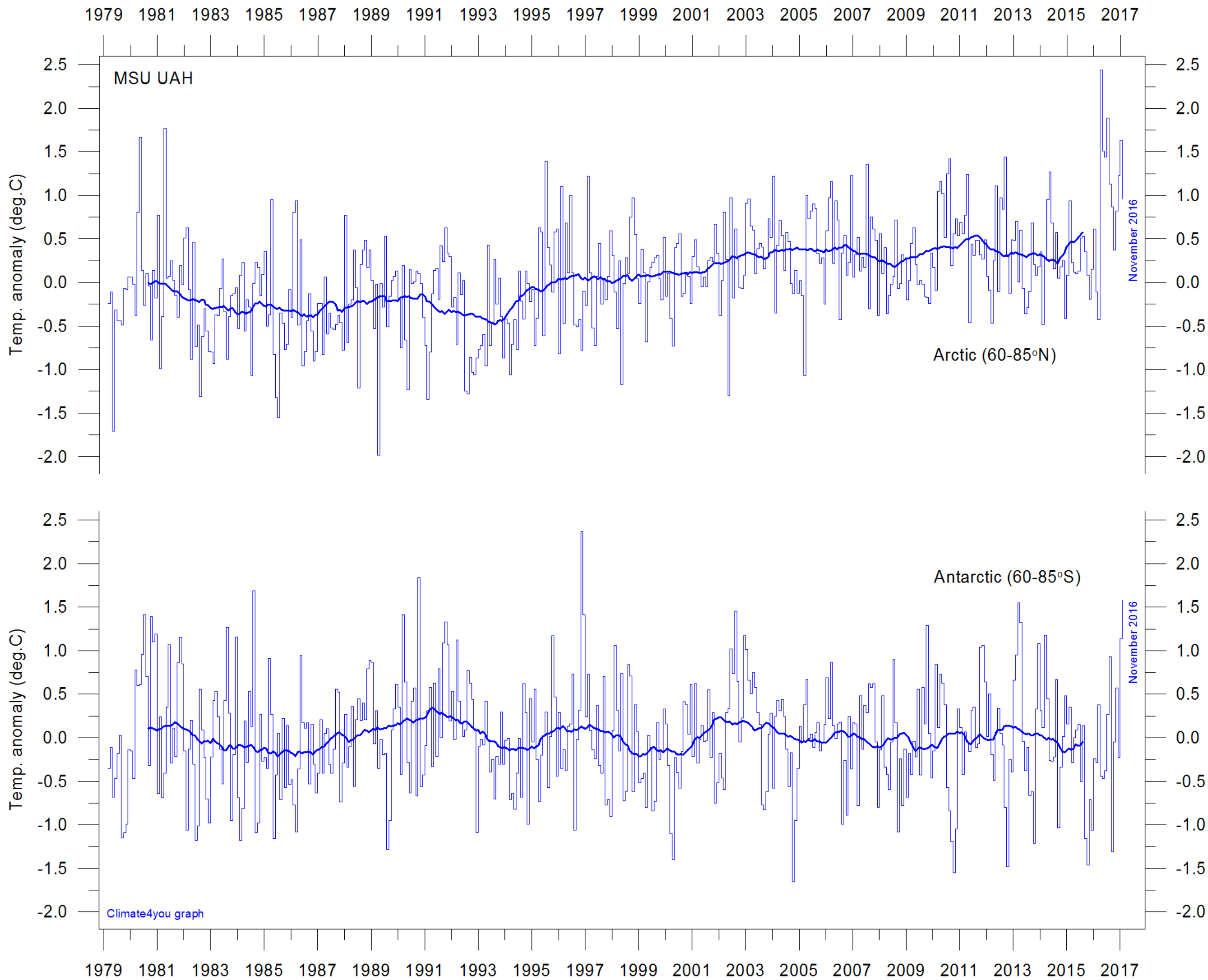

Global monthly average lower troposphere temperature since 1979 for the North Pole and South Pole regions, based on satellite observations (University of Alabama at Huntsville, USA). Thin lines show the monthly temperature. The thick line is the simple running 37-month average, nearly corresponding to a running 3 year average. Reference period 1981-2010.

Arctic and Antarctic surface air temperature, updated to October 2016

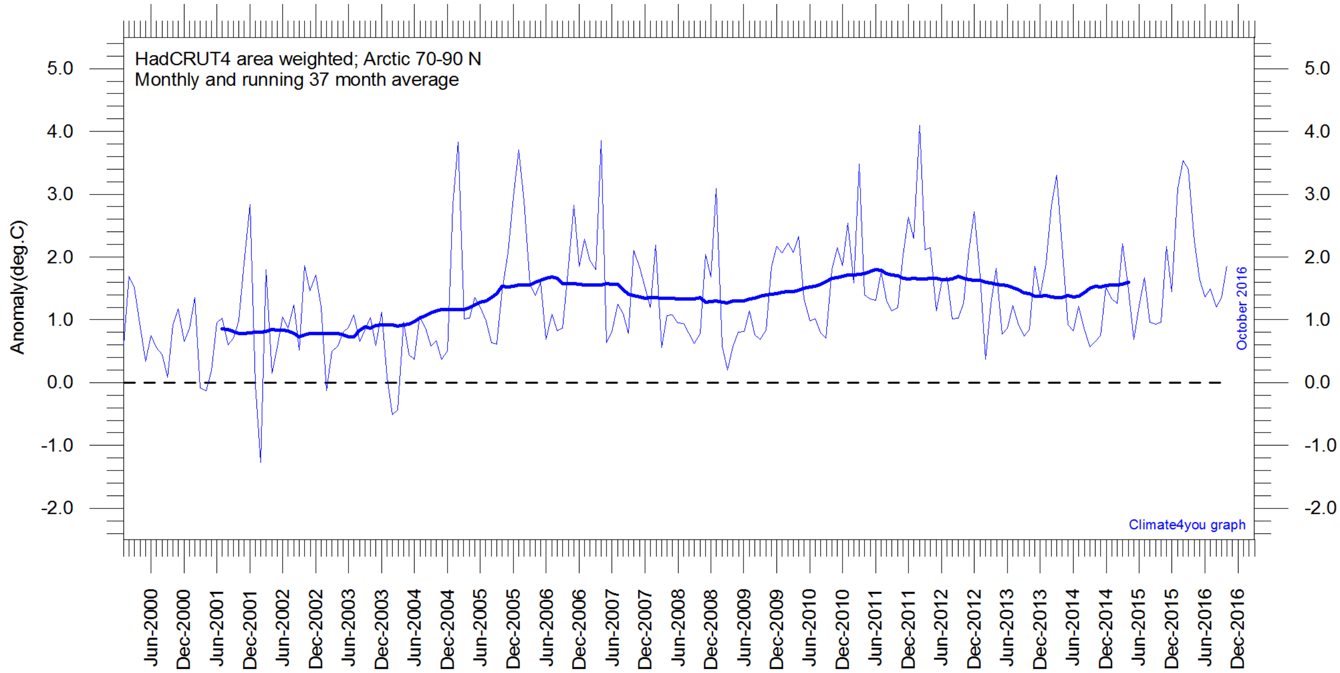

Diagram showing area weighted Arctic (70-90°N) monthly surface air temperature anomalies (HadCRUT4) since January 2000, in relation to the WMO normal period 1961-1990. The thin line shows the monthly temperature anomaly, while the thicker line shows the running 37 month (c. 3 year) average.

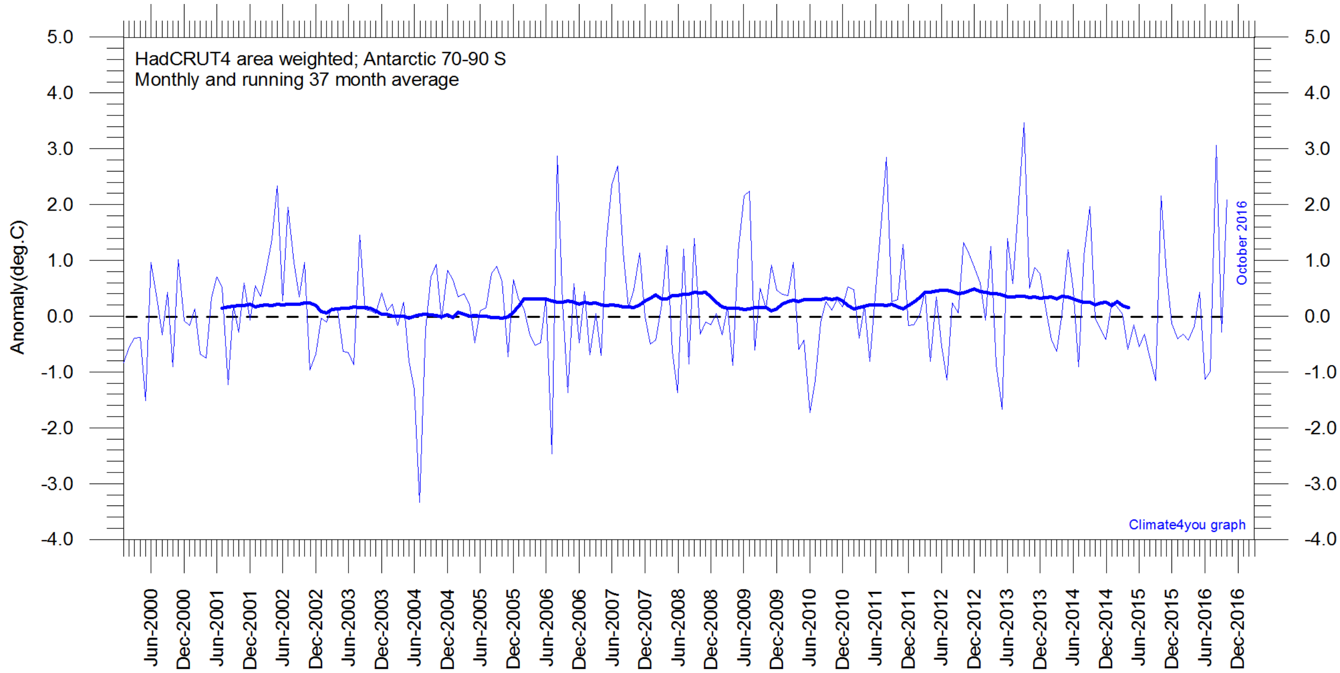

Diagram showing area weighted Antarctic (70-90°N) monthly surface air temperature anomalies (HadCRUT4) since January 2000, in relation to the WMO normal period 1961-1990. The thin line shows the monthly temperature anomaly, while the thicker line shows the running 37 month (c. 3 year) average.

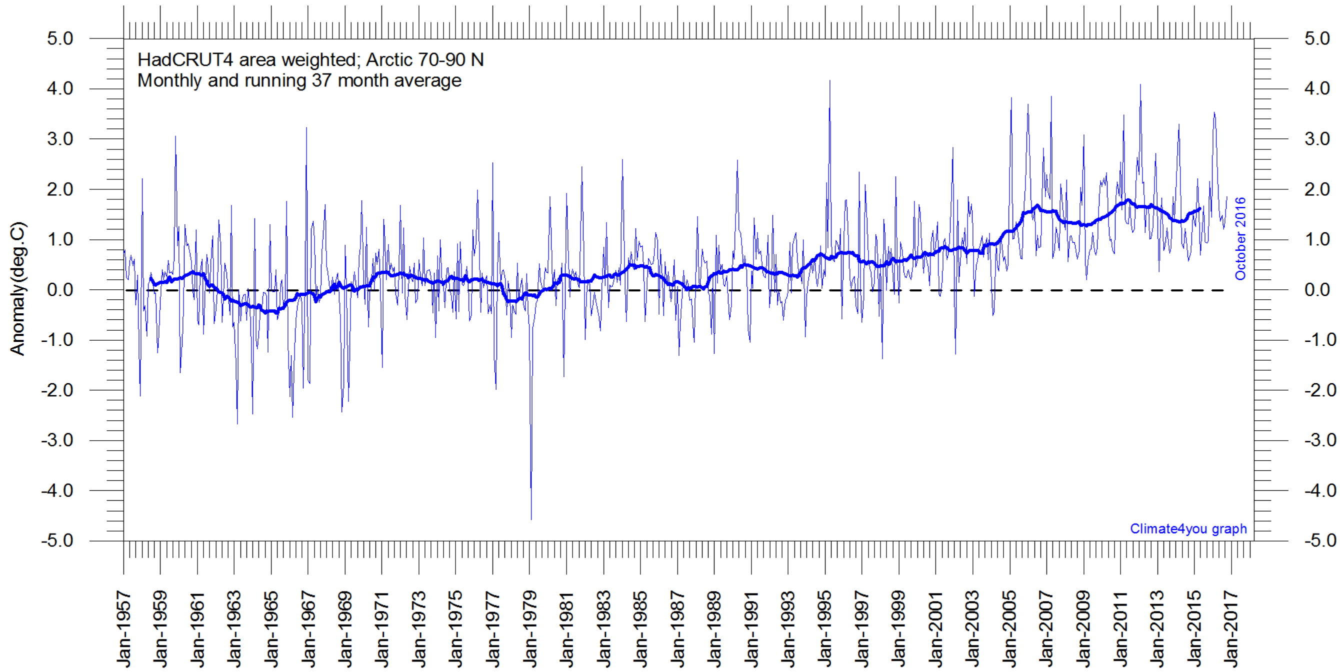

Diagram showing area weighted Arctic (70-90°N) monthly surface air temperature anomalies ([HadCRUT4]) since January 1957, in relation to the WMO [normal period] 1961-1990. The thin line shows the monthly temperature anomaly, while the thicker line shows the running 37 month (c. 3 year) average.

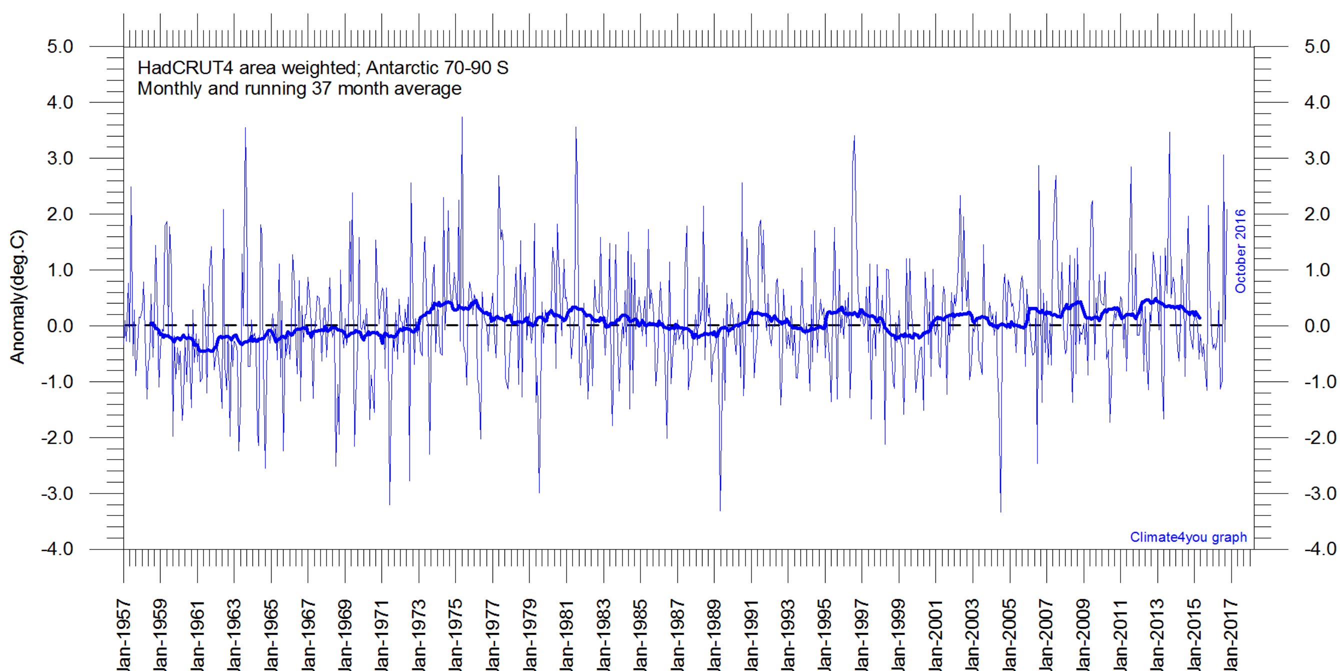

Diagram showing area weighted Antarctic (70-90°N) monthly surface air temperature anomalies ([HadCRUT4]) since January 1957, in relation to the WMO [normal period] 1961-1990. The thin line shows the monthly temperature anomaly, while the thicker line shows the running 37 month (c. 3 year) average.

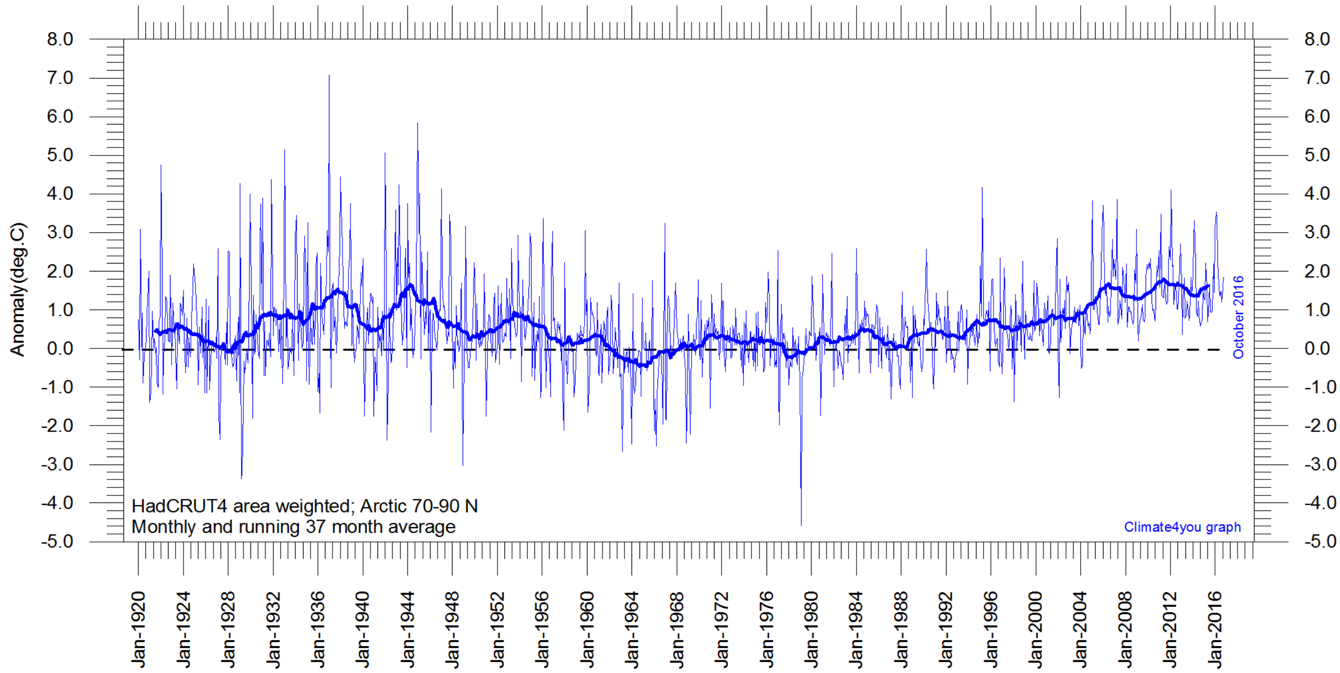

Diagram showing area-weighted Arctic (70-90°N) monthly surface air temperature anomalies ([HadCRUT4]) since January 1920, in relation to the WMO [normal period] 1961-1990. The thin line shows the monthly temperature anomaly, while the thicker line shows the running 37 month (c. 3 year) average. Because of the relatively small number of Arctic stations before 1930, month-to-month variations in the early part of the temperature record are larger than later. The period from about 1930 saw the establishment of many new Arctic meteorological stations, first in Russia and Siberia, and following the 2nd World War, also in North America. The period since 2000 is warm, about as warm as the period 1930-1940.

As the HadCRUT4 data series has improved high latitude coverage data coverage (compared to the HadCRUT3 series) the individual 5°x5° grid cells has been weighted according to their surface area. This is in contrast to Gillet et al. 2008 which calculated a simple average, with no consideration to the surface area represented by the individual 5°x5° grid cells.

Literature:

Gillett, N.P., Stone, D.A., Stott, P.A., Nozawa, T., Karpechko, A.Y.U., Hegerl, G.C., Wehner, M.F. and Jones, P.D. 2008. Attribution of polar warming to human influence. *Nature Geoscience* 1, 750-754.

Arctic and Antarctic sea ice, updated to November 2016

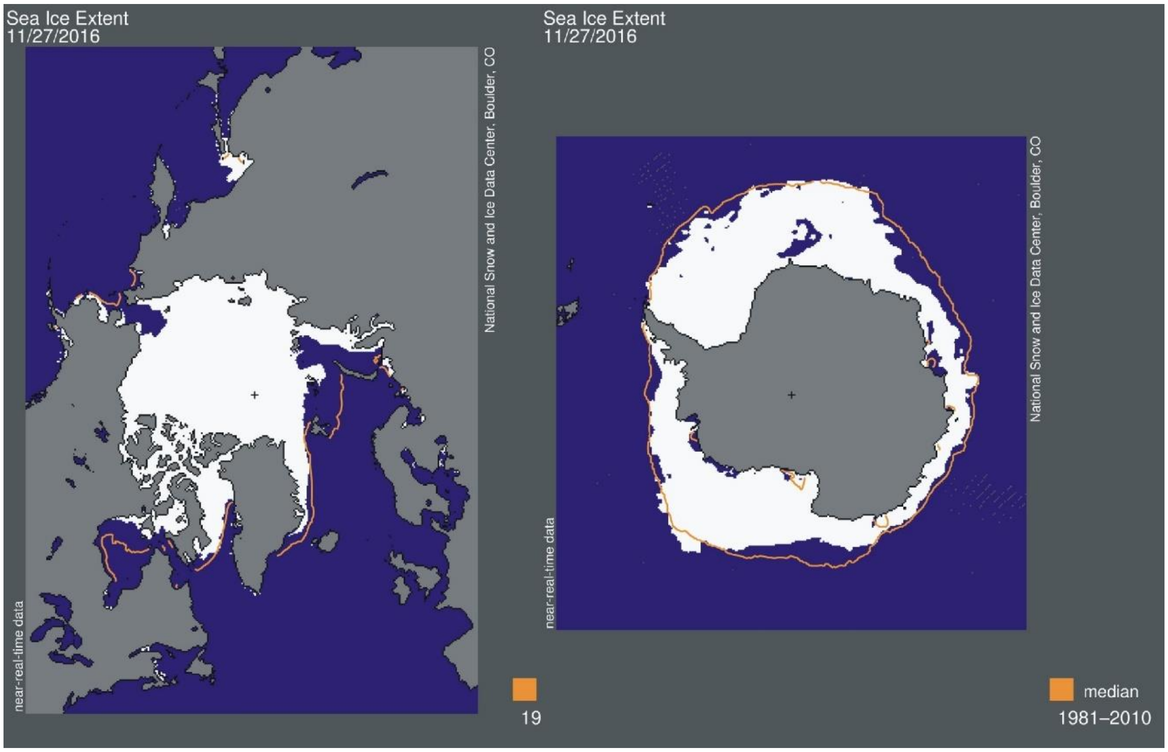

Sea ice extent 27 November 2016. The median limit of sea ice (orange line) is defined as 15% sea ice cover, according to the average of satellite observations 1981-2010 (both years inclusive). Sea ice may therefore well be encountered outside and open water areas inside the limit shown in the diagrams above. Map source: National Snow and Ice Data Center (NSIDC).

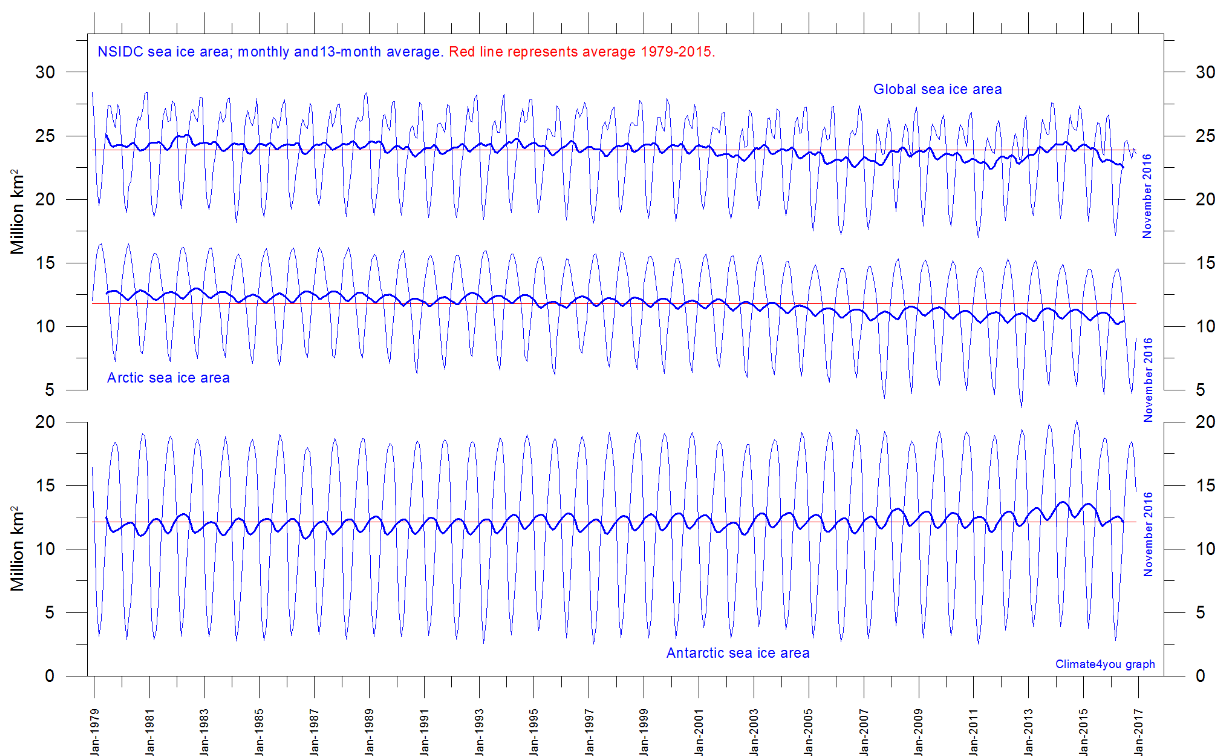

Graphs showing monthly Antarctic, Arctic and global sea ice extent since November 1978, according to the [National Snow and Ice data Center](#) (NSIDC).

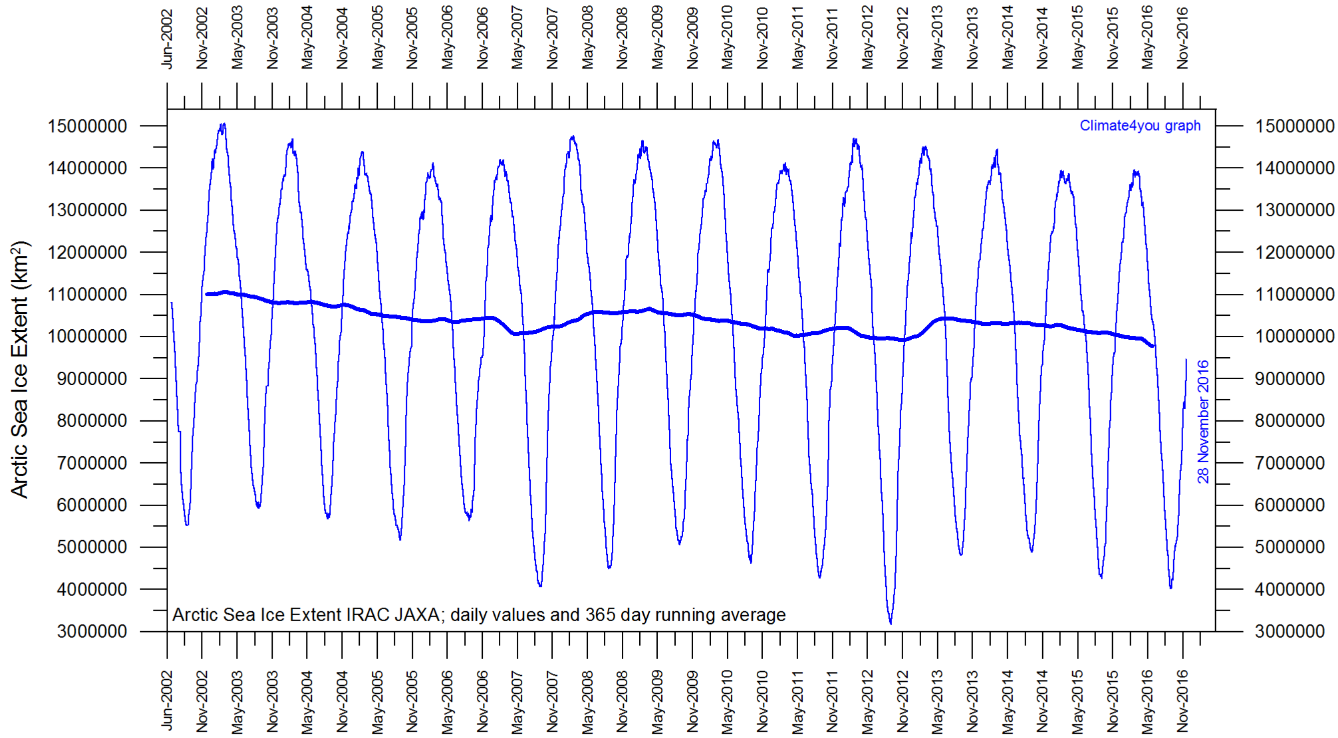

Diagram showing daily Arctic sea ice extent since June 2002, to 28 November 2016, by courtesy of [Japan Aerospace Exploration Agency](#) (JAXA).

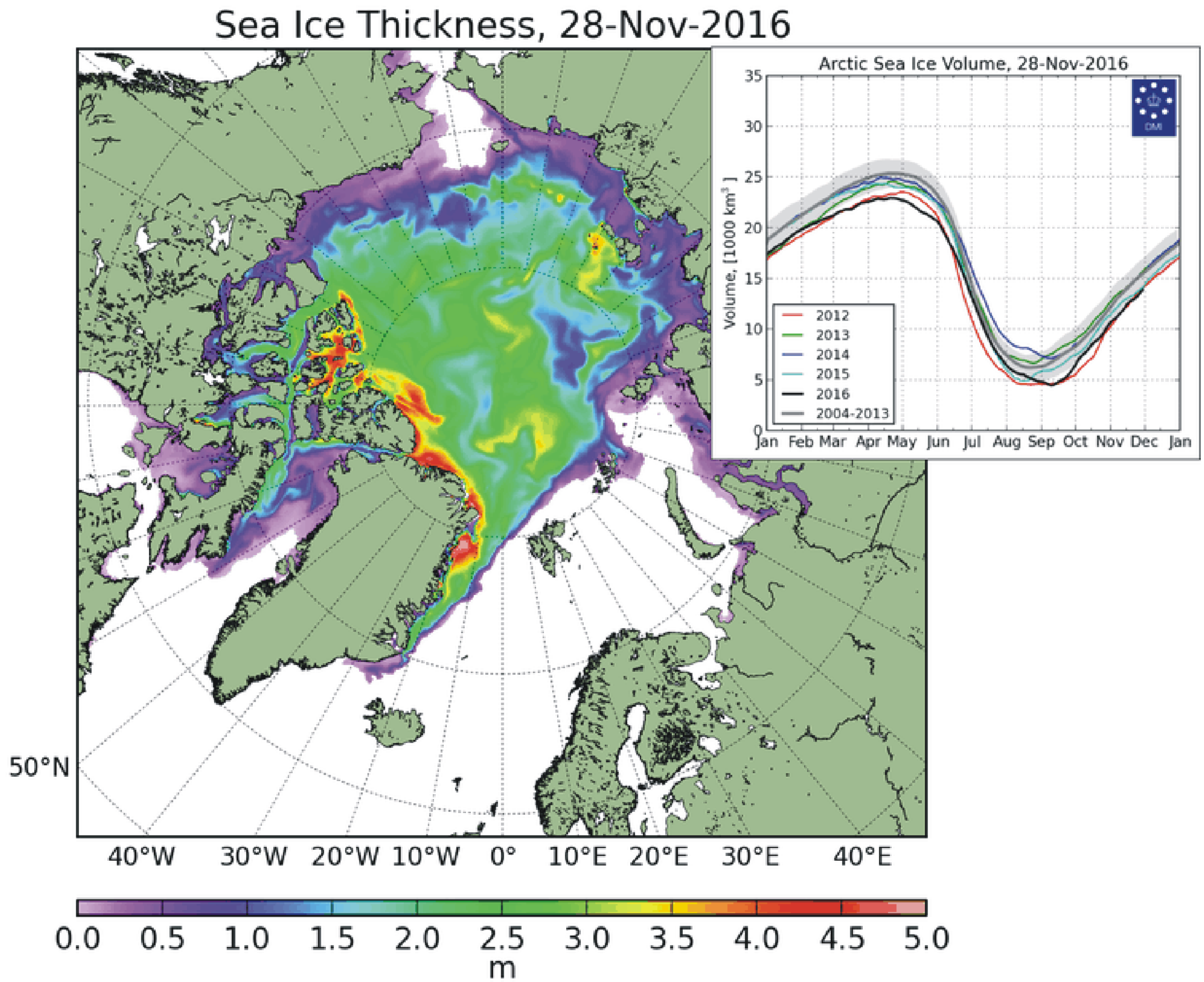

Diagrams showing Arctic sea ice extent 28 November 2016 and the seasonal cycles of the calculated total arctic sea ice volume, according to [The Danish Meteorological Institute (DMI)](). The mean sea ice volume and standard deviation for the period 2004-2013 are shown by gray shading.

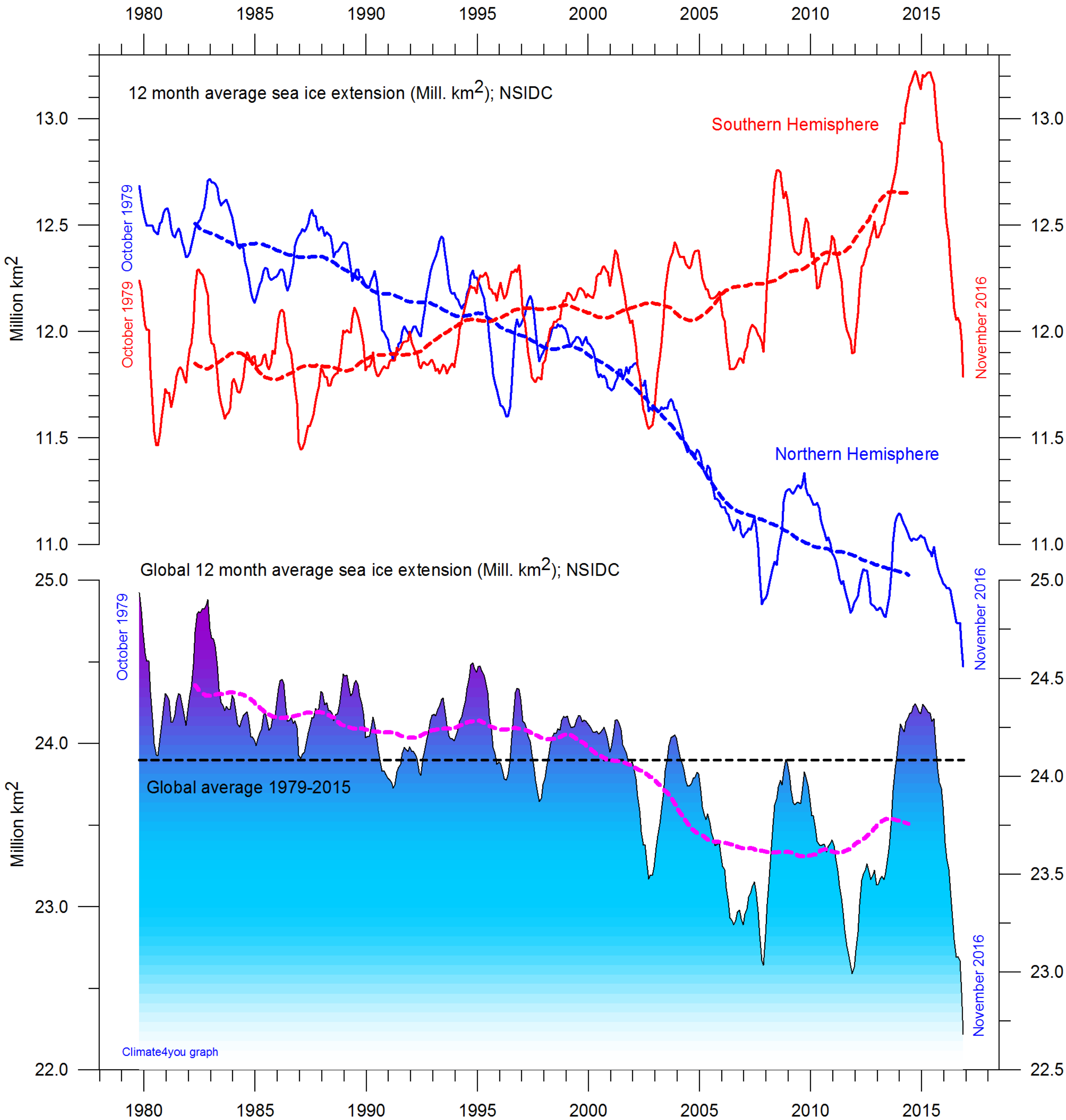

12 month running average sea ice extension, global and in both hemispheres since 1979, the satellite-era. The October 1979 value represents the monthly 12-month average of November 1978 - October 1979, the November 1979 value represents the average of December 1978 - November 1979, etc. The stippled lines represent a 61-month (ca. 5 years) average. Data source: National Snow and Ice Data Center (NSIDC).

Sea level in general

Global (or eustatic) sea-level change is measured relative to an idealised reference level, the geoid, which is a mathematical model of planet Earth's surface (Carter et al. 2014). Global sea-level is a function of the volume of the ocean basins and the volume of water they contain. Changes in global sea-level are caused by – but not limited to - four main mechanisms:

1. Changes in local and regional air pressure and wind, and tidal changes introduced by the Moon.
2. Changes in ocean basin volume by tectonic (geological) forces.
3. Changes in ocean water density caused by variations in currents, water temperature and salinity.
4. Changes in the volume of water caused by changes in the mass balance of terrestrial glaciers.

In addition to these there are other mechanisms influencing sea-level; such as storage of ground water, storage in lakes and rivers, evaporation, etc.

Mechanism 1 is controlling sea-level at many sites on a time scale from months to several years. As an example, many coastal stations show a pronounced annual variation reflecting seasonal changes in air pressures and wind speed. Longer-term climatic changes playing out over decades or centuries will also affect measurements of sea-level changes. Hansen et al. (2011, 2015) provide excellent analyses of sea-level changes caused by recurrent changes of the orbit of the Moon and other phenomena.

Mechanism 2 – with the important exception of earthquakes and tsunamis - typically operates over long (geological) time scales, and is not significant on human time scales. It may relate to variations in the sea-floor spreading rate, causing volume changes in mid-ocean mountain ridges, and to the slowly changing configuration of land and oceans. Another effect may be the slow rise of basins due to isostatic offloading by deglaciation after an ice age. The floor of the Baltic Sea and the Hudson Bay are presently rising, causing a slow net transfer of water from these basins into the adjoining oceans. Slow changes of very big glaciers (ice sheets) and movements in the mantle will affect the gravity field and thereby the vertical position of the ocean surface. Any increase of the total water mass as well as sediment deposition into oceans increase the load on their bottom, generating sinking by viscoelastic flow in the mantle below. The mantle flow is directed towards the surrounding land areas, which will rise, thereby partly compensating for the initial sea level increase induced by the increased water mass in the ocean.

Mechanism 3 (temperature-driven expansion) only affects the uppermost part of the oceans on human time scales. Usually, temperature-driven changes in density are more important than salinity-driven changes. Seawater is characterised by a relatively small coefficient of expansion, but the effect should however not be overlooked, especially when interpreting satellite altimetry data. Temperature-driven expansion of a column of seawater will not affect the total mass of water within the column considered, and will therefore not affect the potential at the top of the water column. Temperature-driven ocean water expansion will therefore not in itself lead to lateral displacement of water, but only lift the ocean surface locally. Near the coast, where people are living, the depth of water approaches zero, so no temperature-driven expansion will take place here (Mörner 2015). Mechanism 3 is for that reason not important for coastal regions.

Mechanism 4 (changes in glacier mass balance) is an important driver for global sea-level changes along coasts, for human time scales. Volume changes of floating glaciers – ice shelves – has no influence on the global sea-level, just like volume changes of floating sea ice has no influence. Only the mass-balance of grounded or land-based glaciers is important for the global sea-level along coasts.

Summing up: Mechanism 1 and 4 are the most important for understanding sea-level changes along coasts.

References:

Carter R.M., de Lange W., Hansen, J.M., Humlum O., Idso C., Kear, D., Legates, D., Mörner, N.A., Ollier C., Singer F. & Soon W. 2014. Commentary and Analysis on the Whitehead& Associates 2014 NSW Sea-Level Report. Policy Brief, NIPCC, 24. September 2014, 44 pp. http://climatechangereconsidered.org/wp-content/uploads/2014/09/NIPCC-Report-on-NSW-Coastal-SL-9z-corrected.pdf

Hansen, J.-M., Aagaard, T. and Binderup, M. 2011. Absolute sea levels and isostatic changes of the eastern North Sea to central Baltic region during the last 900 years. Boreas, 10.1111/j.1502-3885.2011.00229.x. ISSN 0300–9483.

Hansen, J.-M., Aagaard, T. and Huijpers, A. 2015. Sea-Level Forcing by Synchronization of 56- and 74-YearOscillations with the Moon's Nodal Tide on the Northwest European Shelf (Eastern North Sea to Central Baltic Sea). Journ. Coastal Research, 16 pp.

Mörner, Nils-Axel 2015. Sea Level Changes as recorded in nature itself. Journal of Engineering Research and Applications, Vol.5, 1, 124-129.

Global sea level from satellite altimetry, updated to January 2016

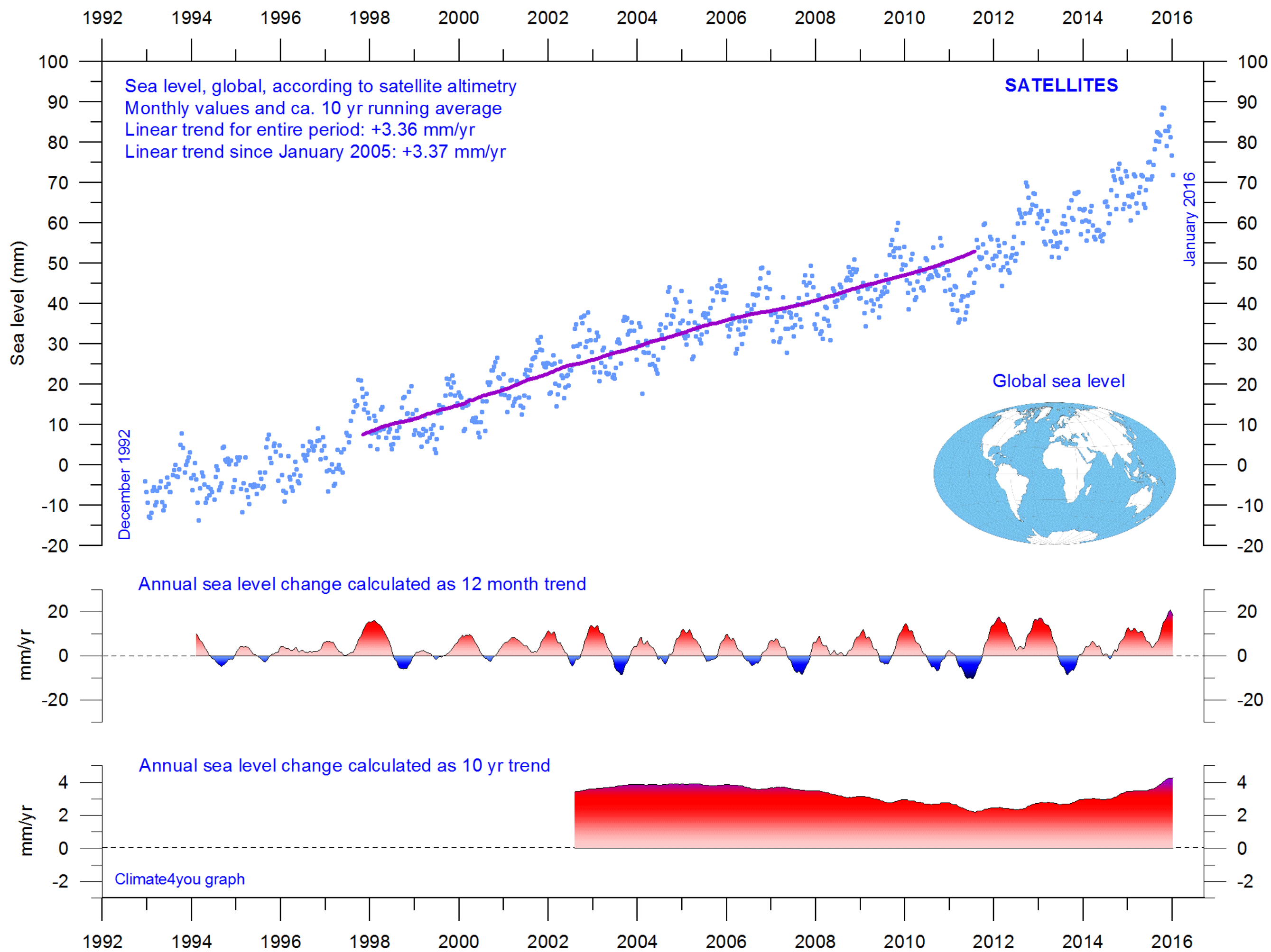

Global sea level since December 1992 according to the Colorado Center for Astrodynamics Research at University of Colorado at Boulder. The blue dots are the individual observations, and the purple line represents the running 121-month (ca. 10 year) average. The two lower panels show the annual sea level change, calculated for 1 and 10 year time windows, respectively. These values are plotted at the end of the interval considered. Data from the TOPEX/Poseidon mission have been used before 2002, and data from the Jason-1 mission (satellite launched December 2001) after 2002.

Global sea level from tide-gauges, updated to December 2015

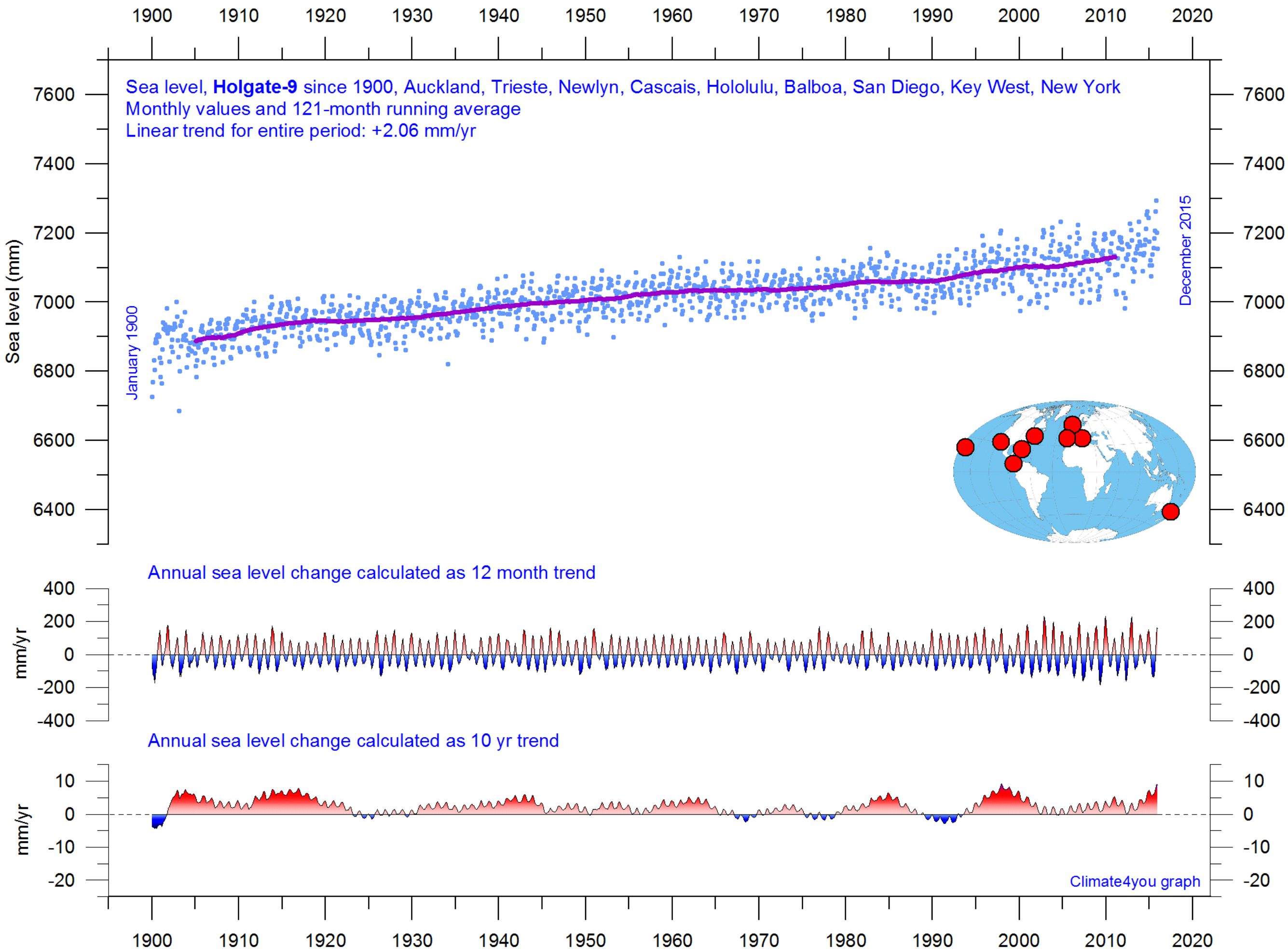

Holgate-9 monthly tide gauge data from PSMSL Data Explorer. Holgate (2007) suggested the nine stations listed in the diagram to capture the variability found in a larger number of stations over the last half century studied previously. For that reason average values of the Holgate-9 group of tide gauge stations are interesting to follow. The blue dots are the individual average monthly observations, and the purple line represents the running 121-month (ca. 10 yr) average. The two lower panels show the annual sea level change, calculated for 1 and 10 yr time windows, respectively. These values are plotted at the end of the interval considered.

Reference:

Holgate, S.J. 2007. On the decadal rates of sea level change during the twentieth century. Geophys. Res. Letters, 34, L01602, doi:10.1029/2006GL028492

Northern Hemisphere weekly snow cover, updated to November 2016

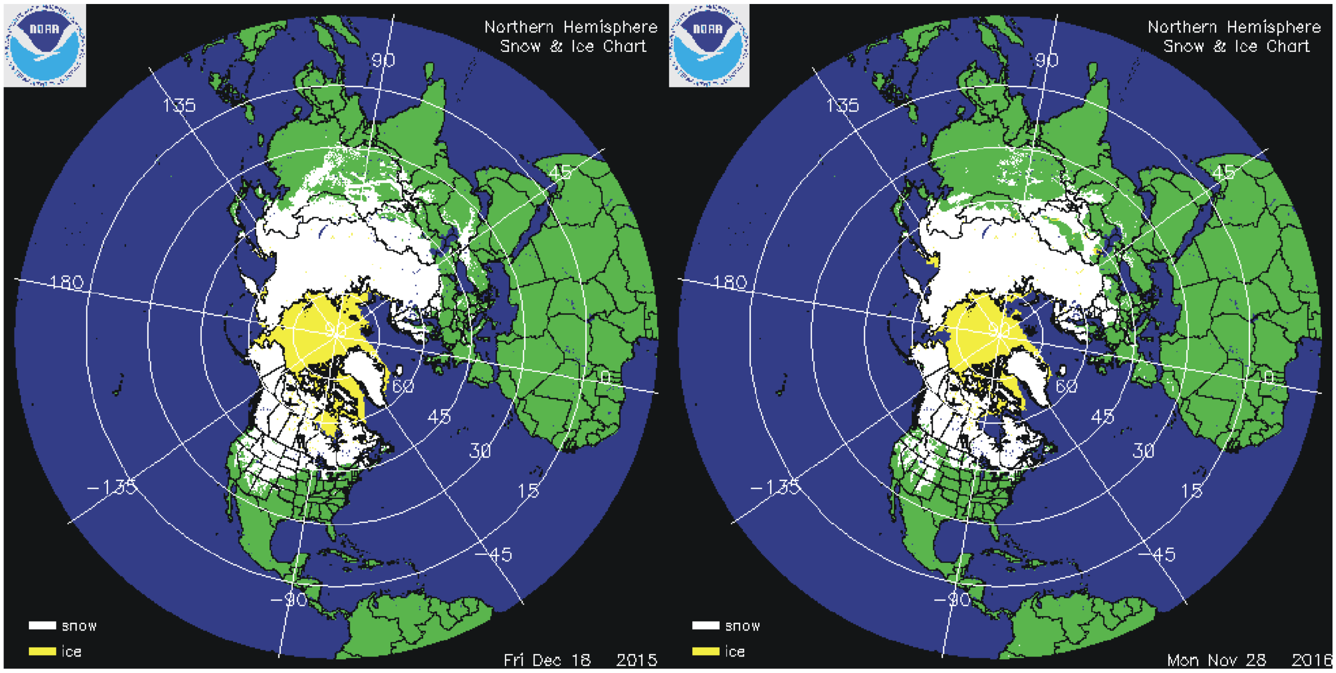

Northern hemisphere snow cover (white) and sea ice (yellow) 28 November 2015 (left) and 2016 (right). Map source: National Ice Center (NIC).

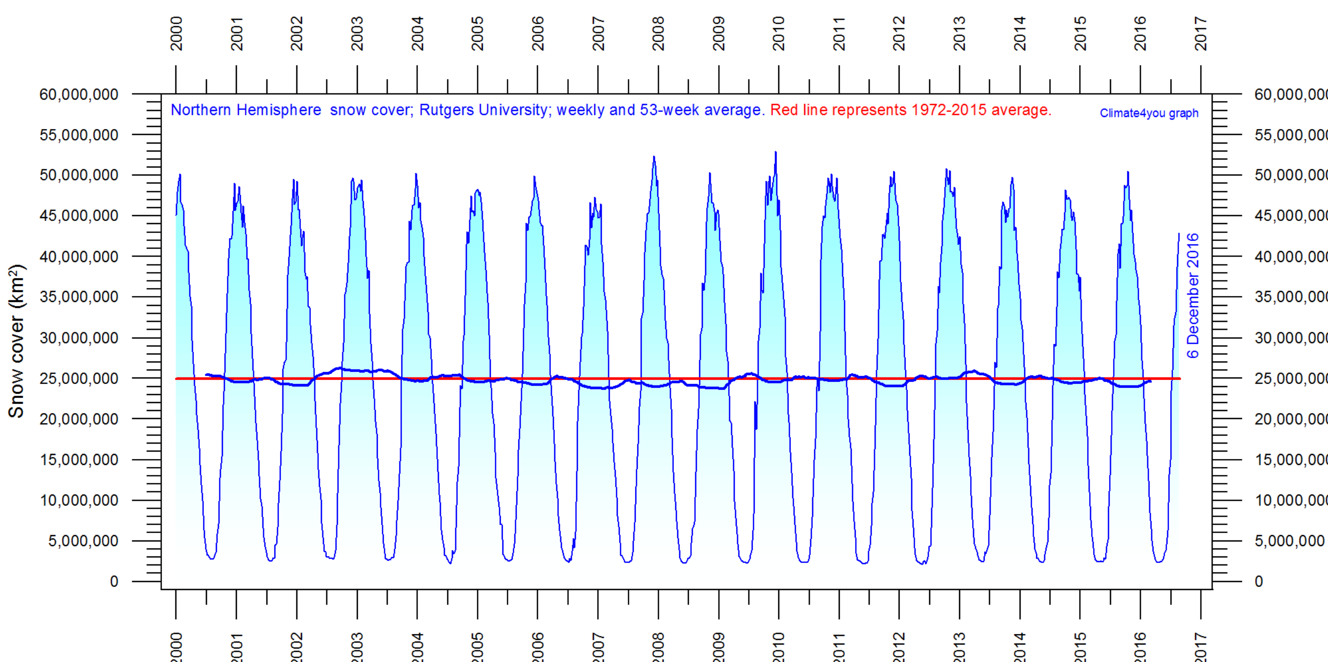

Northern hemisphere weekly snow cover since January 2000 according to Rutgers University Global Snow Laboratory. The thin blue line is the weekly data, and the thick blue line is the running 53-week average (approximately 1 year). The horizontal red line is the 1972-2015 average.

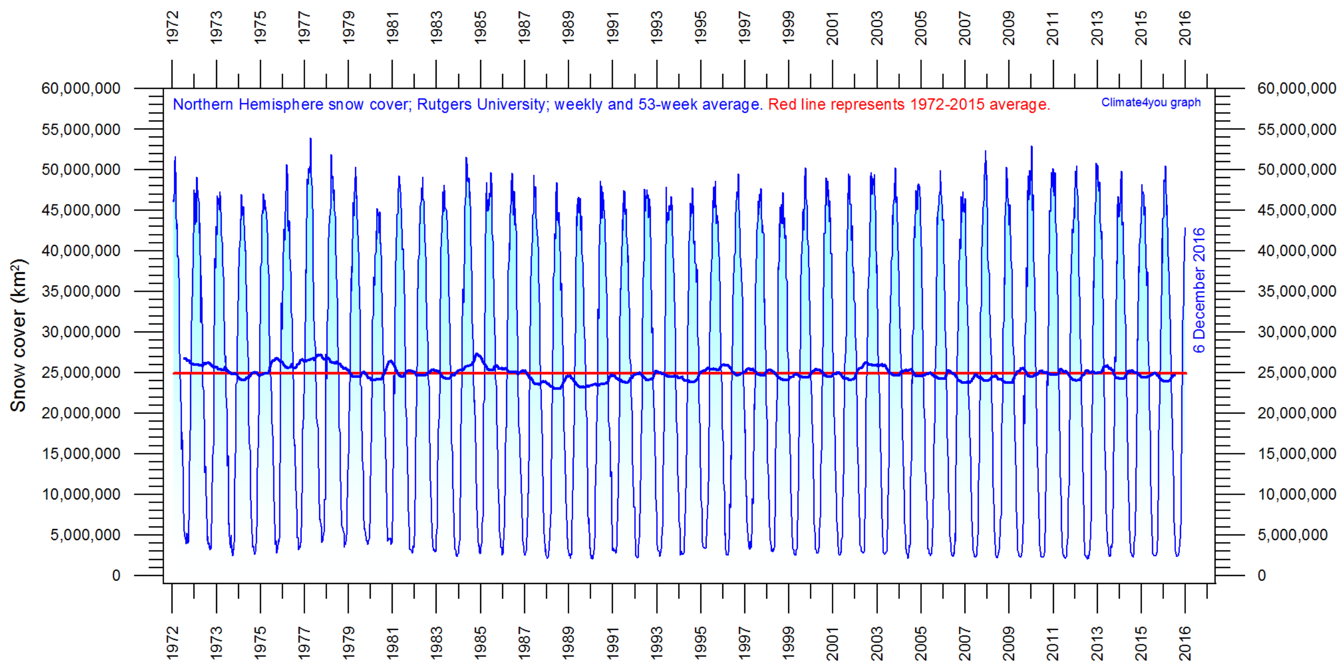

Northern hemisphere weekly snow cover since January 1972 according to Rutgers University Global Snow Laboratory. The thin blue line is the weekly data, and the thick blue line is the running 53-week average (approximately 1 year). The horizontal red line is the 1972-2015 average.

Atmospheric specific humidity, updated to November 2016

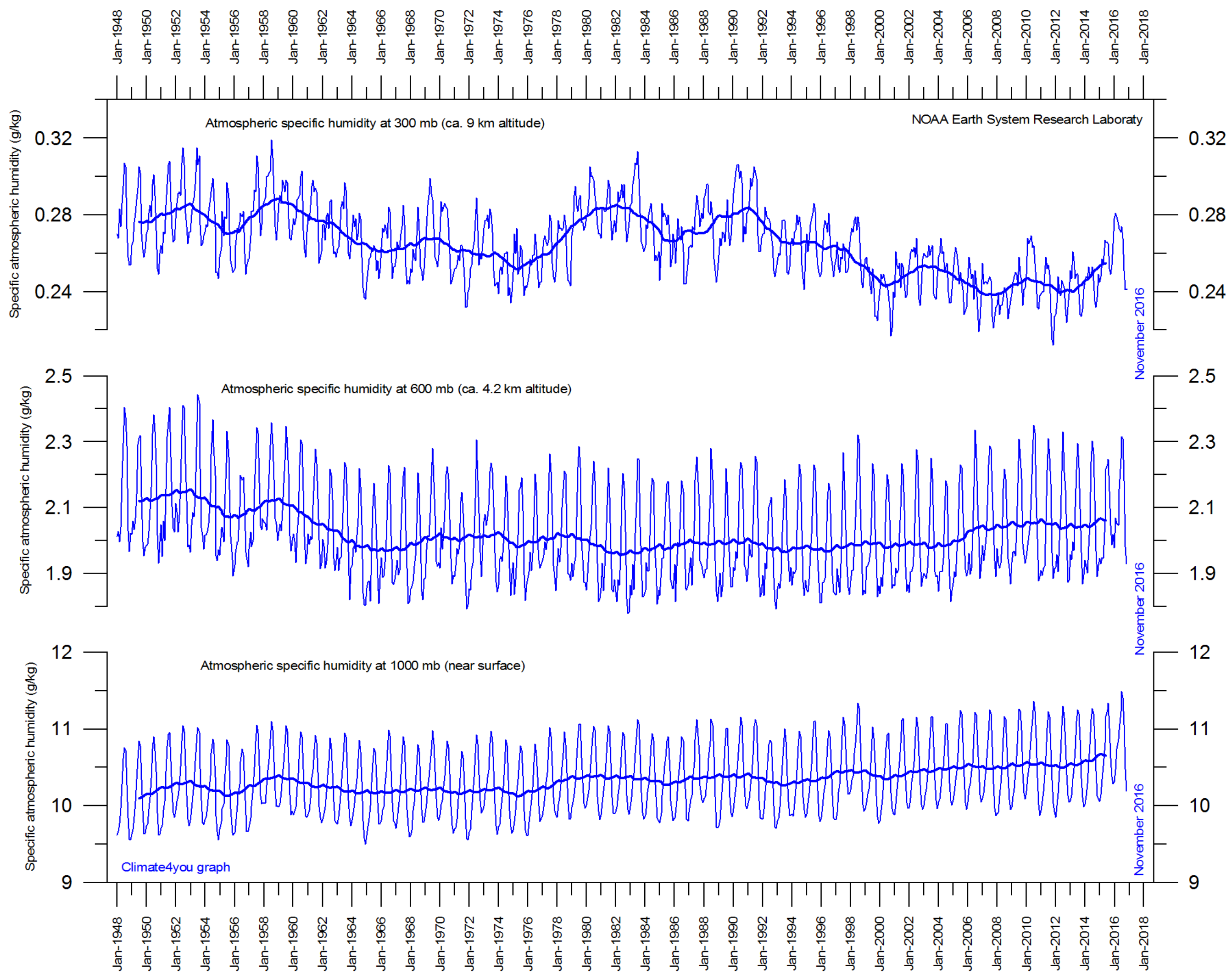

Specific atmospheric humidity (g/kg) at three different altitudes in the lower part of the atmosphere (the Troposphere) since January 1948 (Kalnay et al. 1996). The thin blue lines shows monthly values, while the thick blue lines show the running 37-month average (about 3 years). Data source: Earth System Research Laboratory (NOAA).

Atmospheric CO_2, updated to November 2016

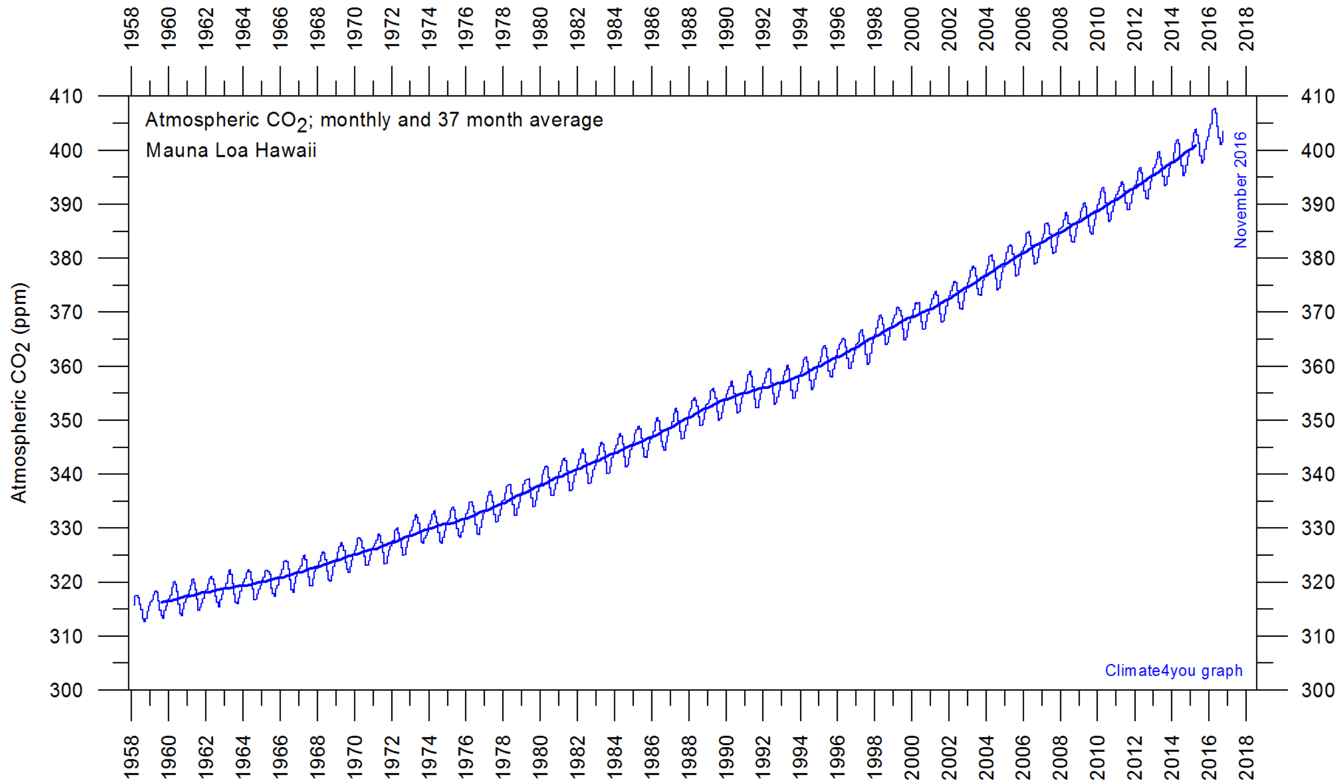

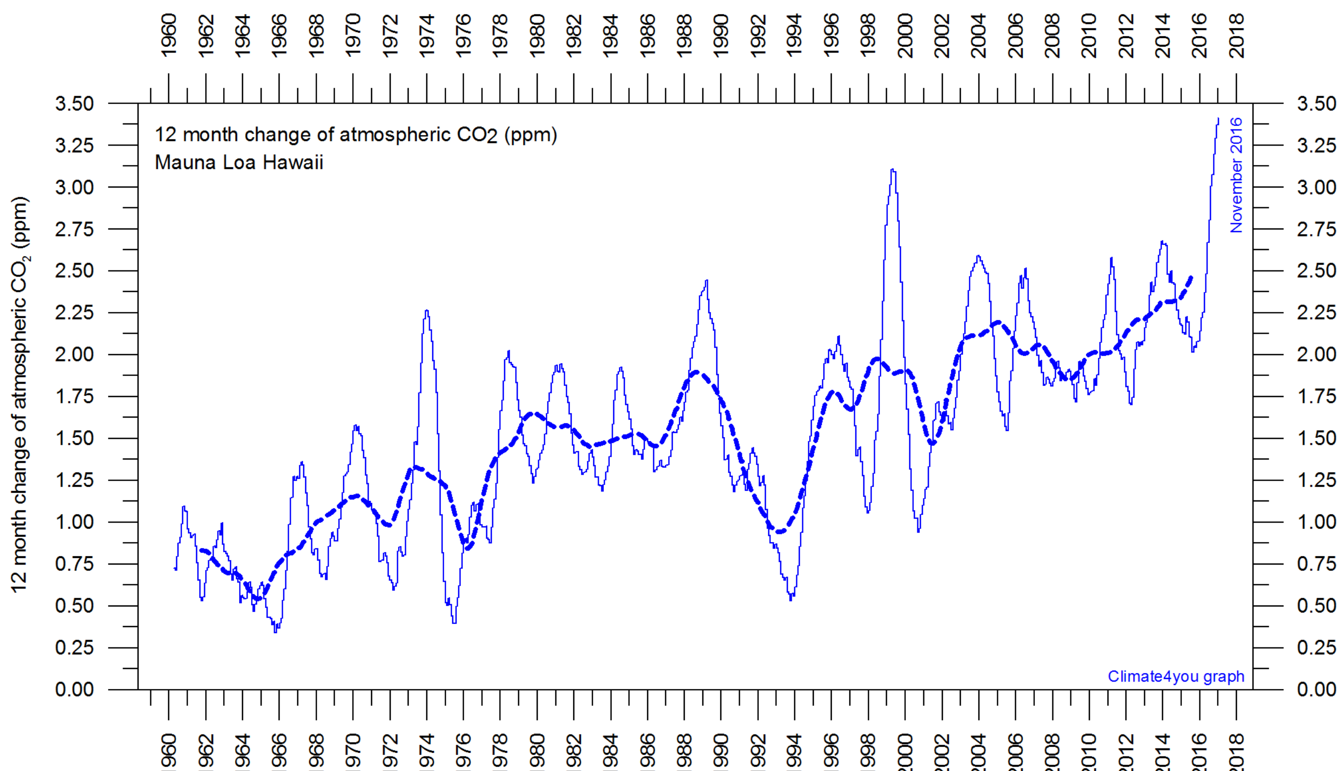

Monthly amount of atmospheric CO_2 (upper diagram) and annual growth rate (lower diagram); average last 12 months minus average preceding 12 months, thin line) of atmospheric CO_2 since 1959, according to data provided by the Mauna Loa Observatory, Hawaii, USA. The thick, stippled line is the simple running 37-observation average, nearly corresponding to a running 3 year average.

The phase relation between atmospheric CO_2 and global temperature, updated to October 2016

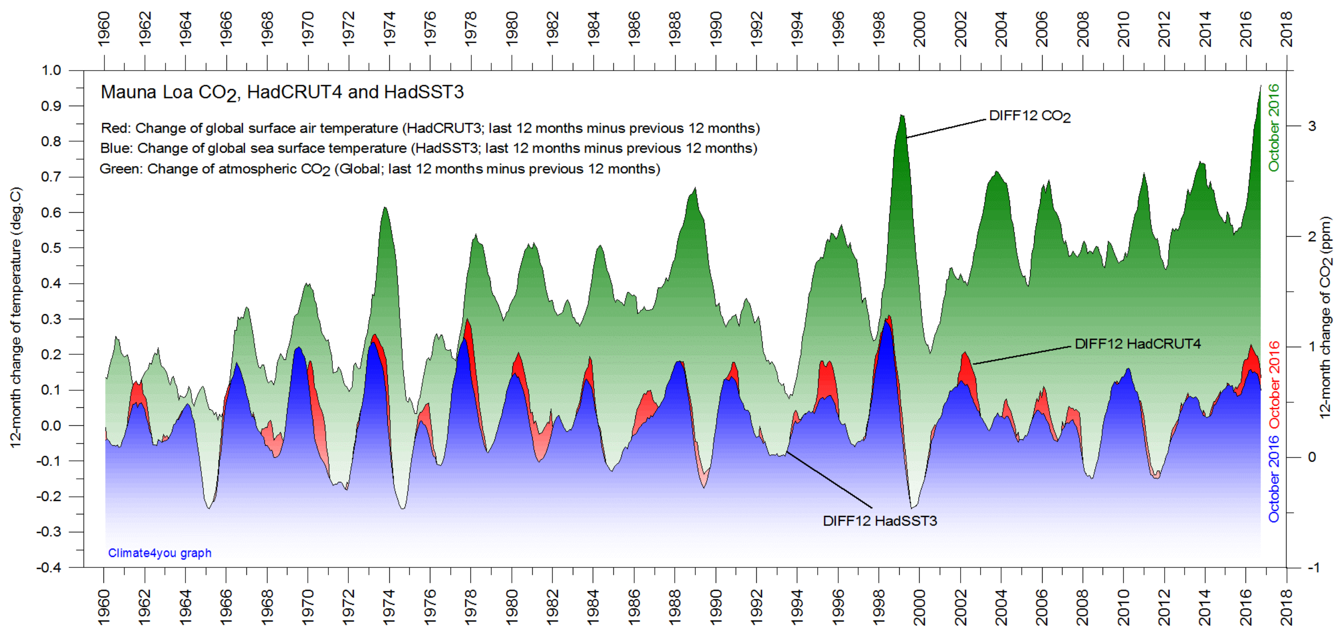

12-month change of global atmospheric CO_2 concentration (Mauna Loa; green), global sea surface temperature (HadSST3; blue) and global surface air temperature (HadCRUT4; red dotted). All graphs are showing monthly values of DIFF12, the difference between the average of the last 12 month and the average for the previous 12 months for each data series.

References:

Humlum, O., Stordahl, K. and Solheim, J-E. 2012. The phase relation between atmospheric carbon dioxide and global temperature. Global and Planetary Change, August 30, 2012. http://www.sciencedirect.com/science/article/pii/S0921818112001658?v=s5

Global surface air temperature and atmospheric CO_2, updated to November 2016

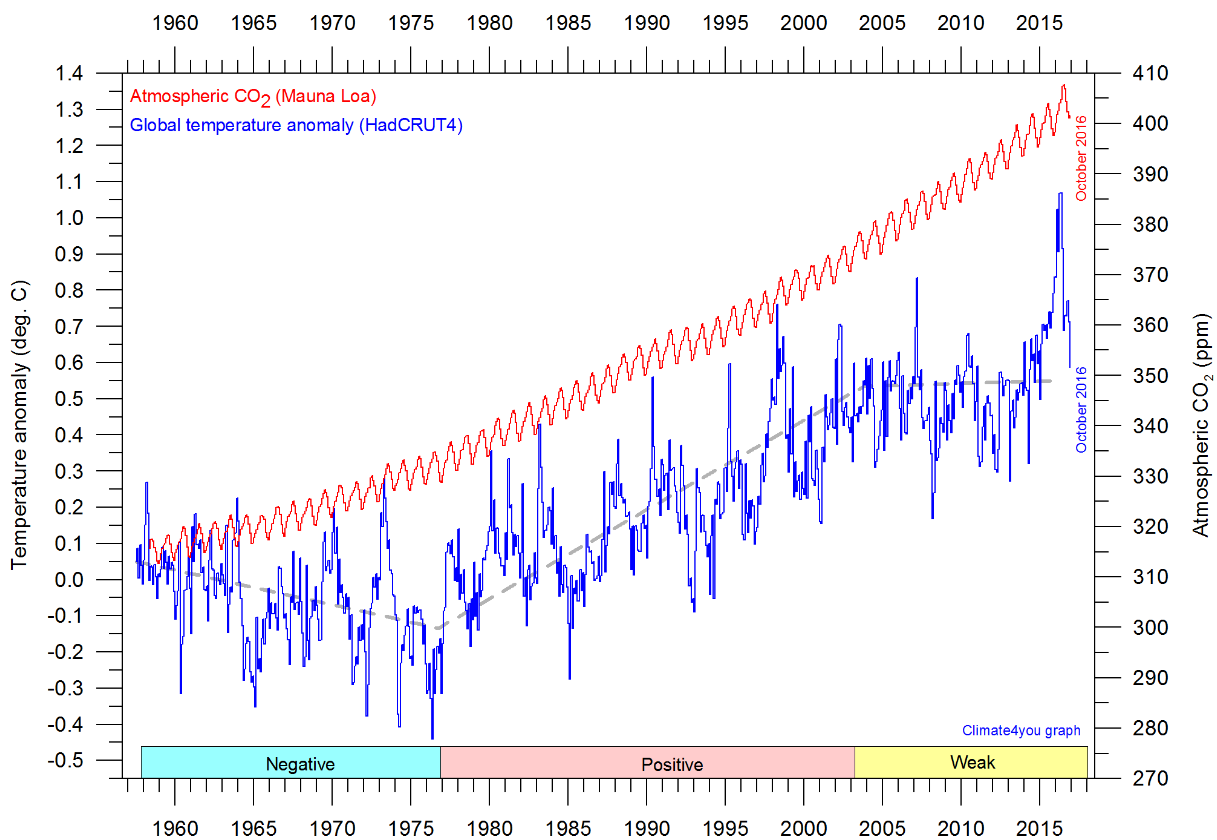

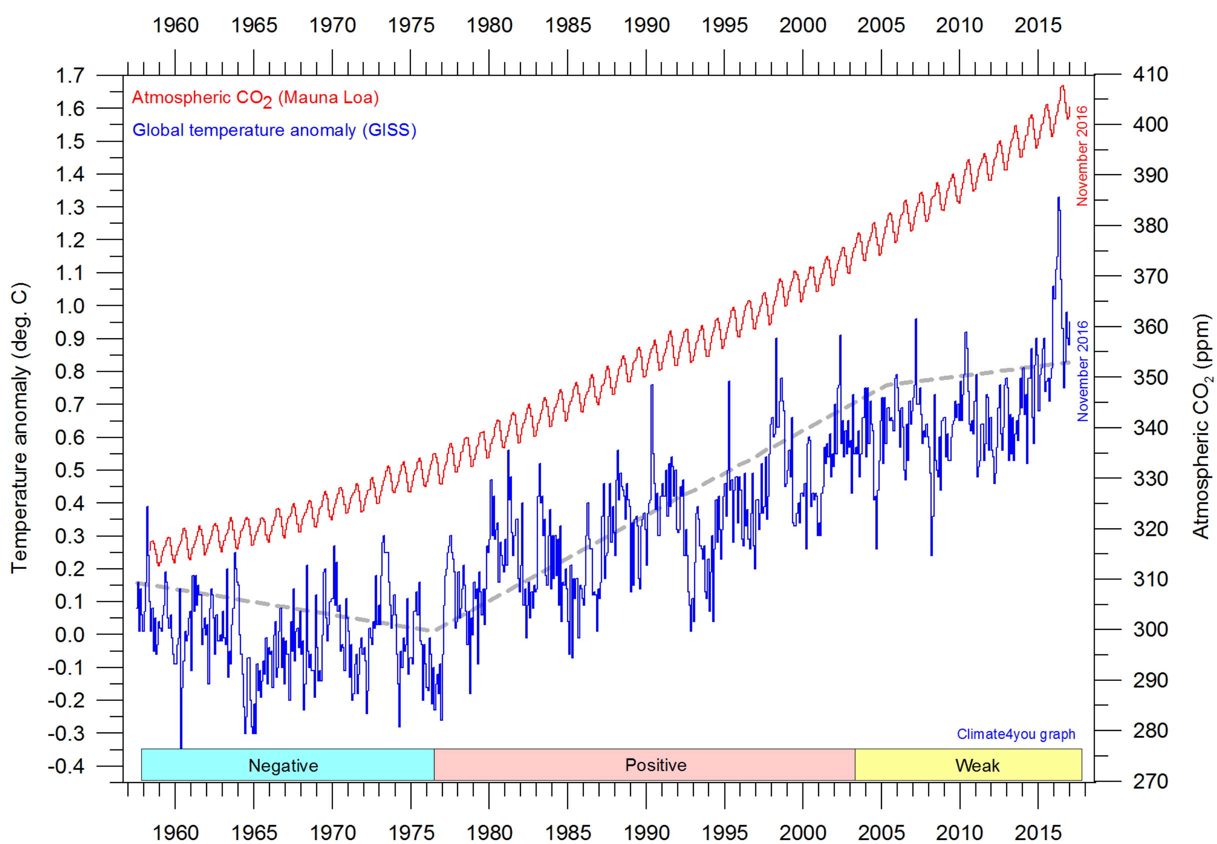

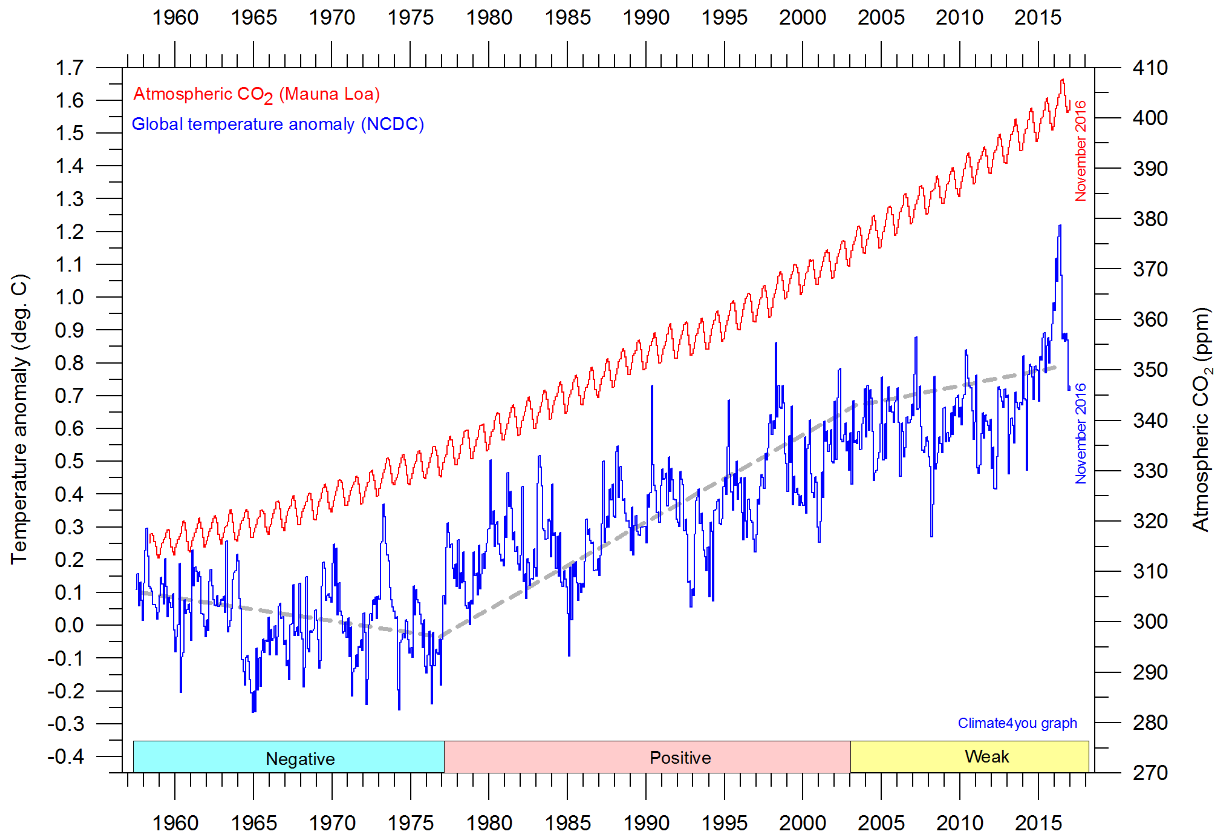

Diagrams showing HadCRUT4, GISS, and NCDC monthly global surface air temperature estimates (blue) and the monthly atmospheric CO_2 content (red) according to the [Mauna Loa Observatory](), Hawaii. The Mauna Loa data series begins in March 1958, and 1958 was therefore chosen as starting year for the diagrams. Reconstructions of past atmospheric CO_2 concentrations (before 1958) are not incorporated in this diagram, as such past CO_2 values are derived by other means (ice cores, stomata, or older measurements using different methodology), and therefore are not directly comparable with direct atmospheric measurements. The dotted grey line indicates the approximate linear temperature trend, and the boxes in the lower part of the diagram indicate the relation between atmospheric CO_2 and global surface air temperature, negative or positive. Please note that the HadCRUT4 diagram is not yet updated beyond October 2016.

Most climate models are programmed to give the greenhouse gas carbon dioxide CO_2 significant influence on global temperature. It is therefore relevant to compare different temperature records with measurements of atmospheric CO_2, as shown in the diagrams above.

Any comparison, however, should not be made on a monthly or annual basis, but for a longer time period, as other effects (oceanographic, etc.) may well override the potential influence of CO_2 on short time scales such as just a few years. It is of cause equally inappropriate to present new meteorological record values, whether daily, monthly or annual, as support for the hypothesis ascribing high importance of atmospheric CO_2 for global temperatures. Any such meteorological record value may well be the result of other phenomena.

What exactly defines the critical length of a relevant time period to consider for evaluating the alleged importance of CO_2 remains elusive and represents a theme for discussion. However, the length of the critical period must be inversely proportional to the temperature sensitivity of CO_2, including feedback effects. If the net temperature effect of atmospheric CO_2 is strong, the critical time period will be short, and vice versa.

However, past climate research history provides some clues as to what has traditionally been considered the relevant length of period over which to compare temperature and atmospheric

CO_2. After about 10 years of concurrent global temperature- and CO_2-increase, IPCC was established in 1988. For obtaining public and political support for the CO_2-hyphotesis the 10-year warming period leading up to 1988 in all likelihood was important. Had the global temperature instead been decreasing, politic support for the hypothesis would have been difficult to obtain.

Based on the previous 10 years of concurrent temperature- and CO_2-increase, many climate scientists in 1988 presumably felt that their understanding of climate dynamics was sufficient to conclude about the importance of CO_2 for global temperature changes. From this it may safely be concluded that 10 years was considered a period long enough to demonstrate the effect of increasing atmospheric CO_2 on global temperatures.

Adopting this approach as to critical time length (at least 10 years), the varying relation (positive or negative) between global temperature and atmospheric CO_2 has been indicated in the lower panels of the diagrams above.

Latest 20-year QC1 global monthly air temperature changes, updated to November 2016

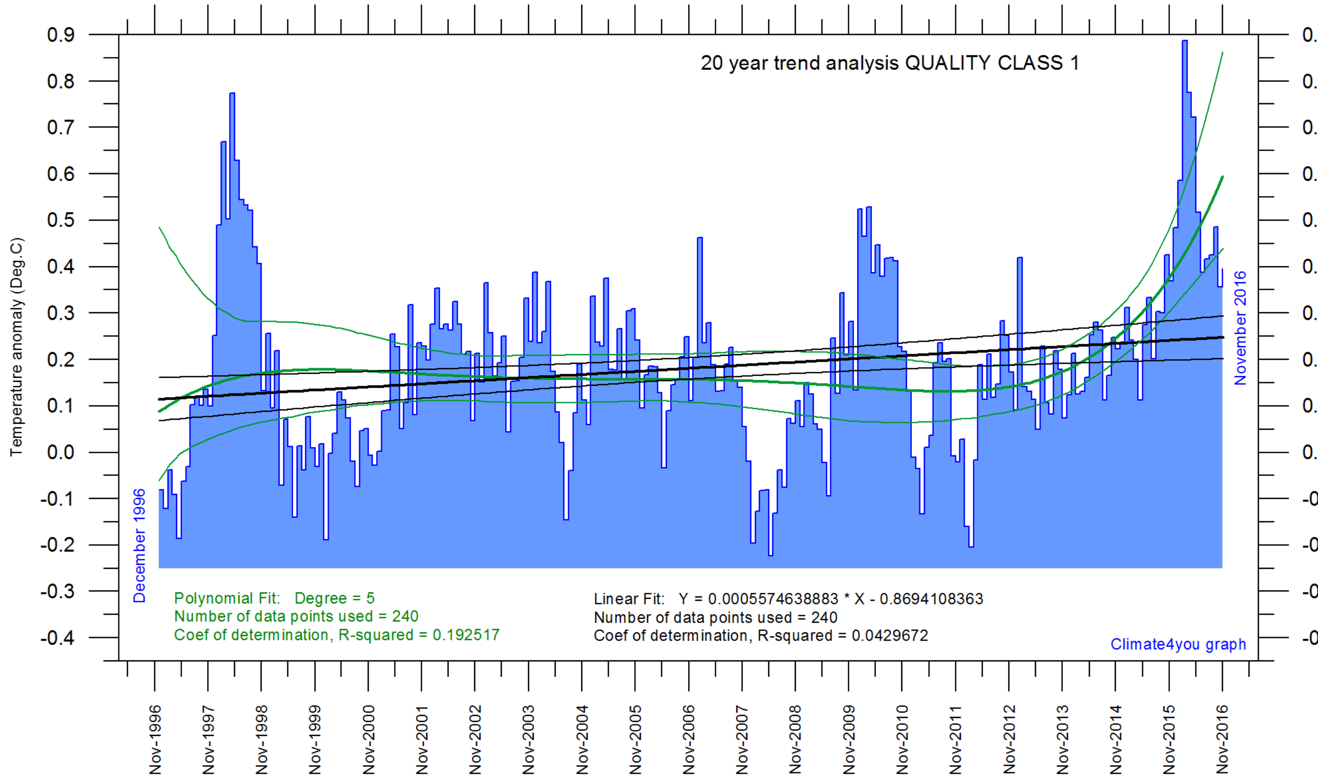

Last 20 years' global monthly average air temperature according to Quality Class 1 (UAH and RSS; see p.10) global monthly temperature estimates. The thin blue line represents the monthly values. The thick black line is the linear fit, with 95% confidence intervals indicated by the two thin black lines. The thick green line represents a 5-degree polynomial fit, with 95% confidence intervals indicated by the two thin green lines. A few key statistics are given in the lower part of the diagram (please note that the linear trend is the monthly trend).

In the ongoing climate debate the question if the global surface air temperature still increases, or if the temperature has levelled out during the last 15-18 years, is often put forward.

The diagram above may be useful in this context, and demonstrates the differences between two often used statistical approaches to determine recent temperature trends. Please also note that such fits only attempt to describe the past, and usually have limited predictive power. In addition, before using any linear trend (or other) analysis of time series a proper statistical model should be chosen, based on statistical justification.

For temperature time series, there is no *a priori* physical reason why the long-term trend should be linear in time. In fact, climatic time series often have trends for which a straight line is not a good approximation, as can clearly be seen from several of the diagrams in the present report.

For an excellent description of problems often encountered by analyses of temperature time series analyses please see Keenan, D.J. 2014: Statistical Analyses of Surface Temperatures in the IPCC Fifth Assessment Report.

Sunspot activity and QC1 average satellite global air temperature, updated to November 2016

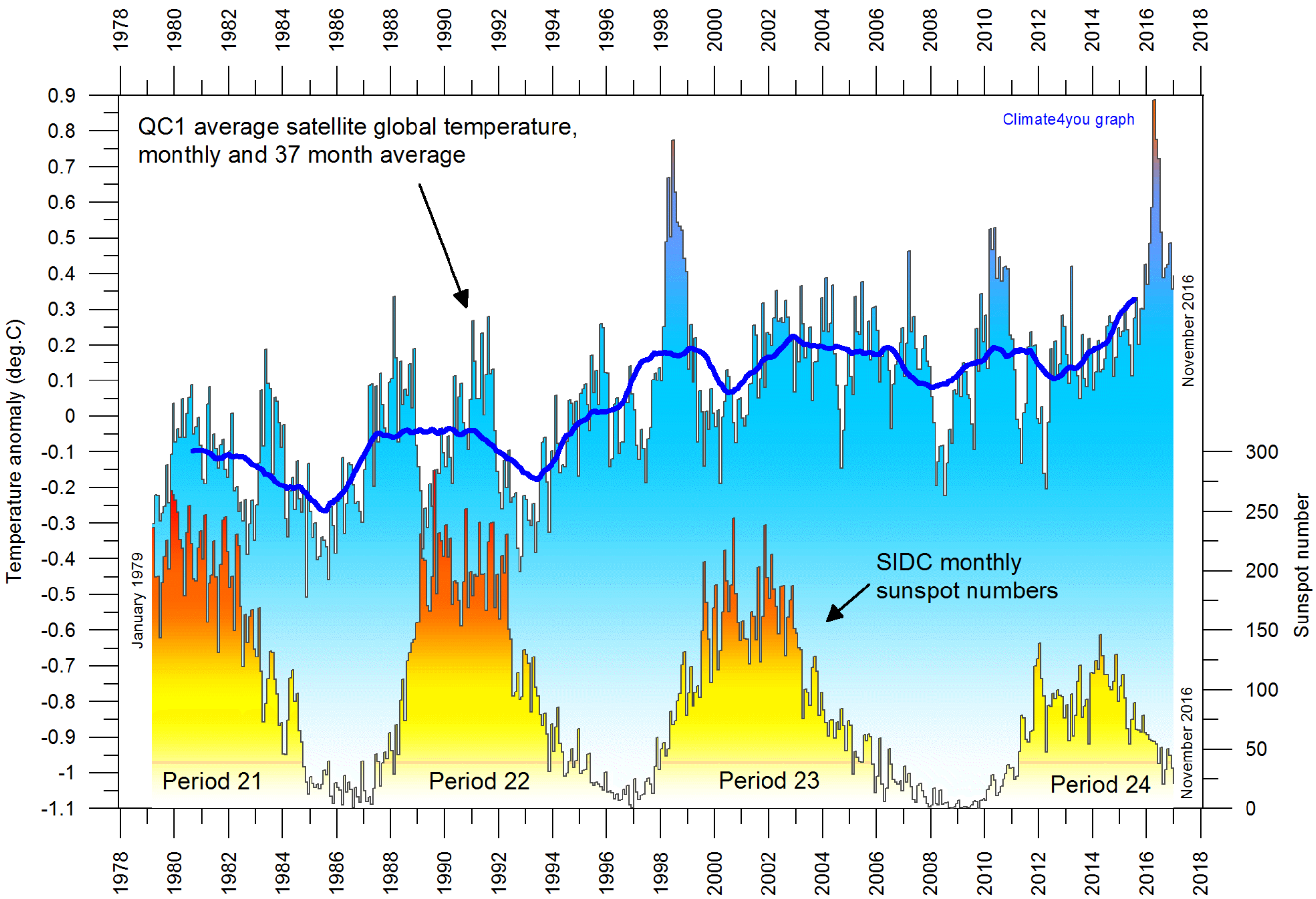

Variation of global monthly air temperature according to Quality Class 1 (UAH and RSS; see p.4) and observed sunspot number as provided by the Solar Influences Data Analysis Center (SIDC), since 1979. The thin lines represent the monthly values, while the thick line is the simple running 37-month average, nearly corresponding to a running 3 yr average. The asymmetrical temperature 'bump' around 1998 is influenced by the oceanographic El Niño phenomenon in 1998, as is the case also for 2015-16.

Climate and history; one example among many

1783-1784: The Laki eruption in Iceland

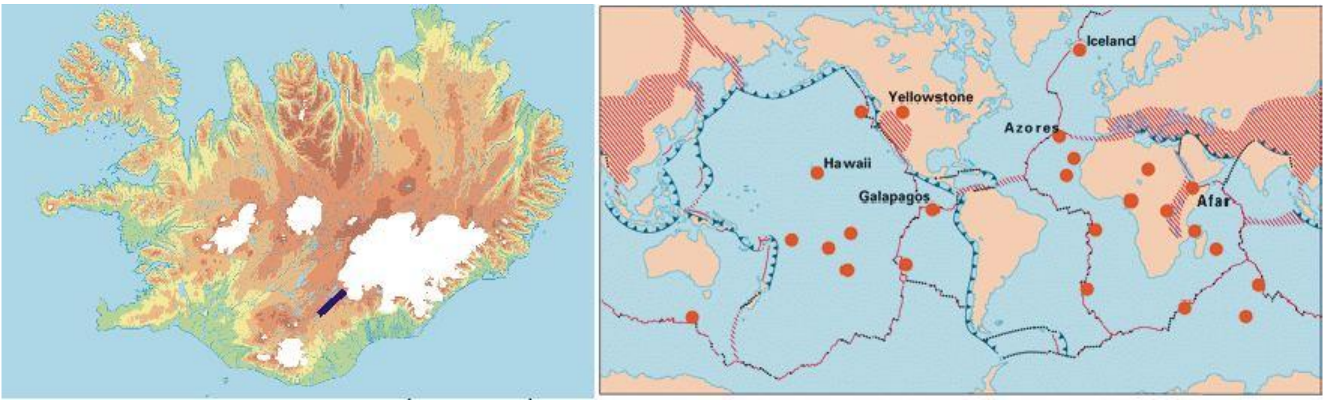

Topographic map showing Iceland with the Laki fissure indicated by a black line (left). Geological plate boundaries and hotspots (red dots) on planet Earth (right).

Laki or Lakagígar (Craters of Laki) is a volcanic fissure in southern Iceland, which has been active several times in historical time. In year 1783 Laki erupted together with the adjoining Grímsvötn volcano in the large ice cap Vatnajökull, killing more than 50% of the livestock, and leading to a famine which killed about 21% of the total population in Iceland.

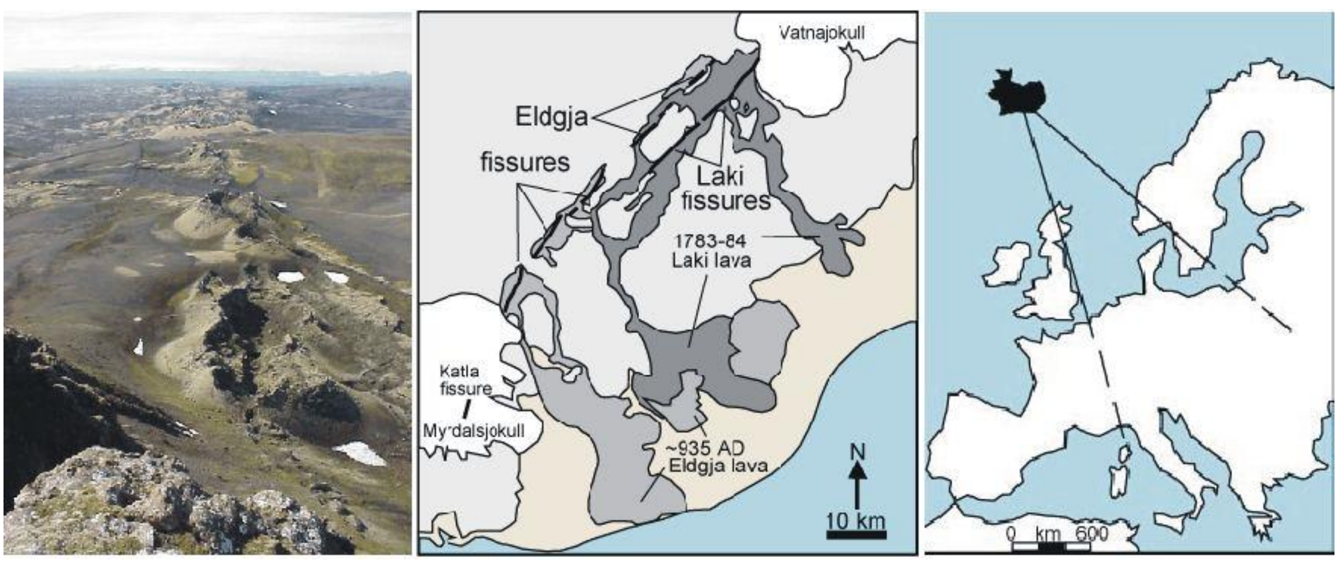

Volcanic craters along the Laki fissure in southern Iceland (left). Map showing extent of lava streams derived from the Laki eruption in 1783-1784 and the previous Eldgja eruption in year 935 (centre). Map showing regions in Europe affected by ash fall from the Laki eruption (right).

The eruption started on June 8, 1783, with about 130 craters along the fissure erupting explosively, because the rising lava met huge amounts of ground water on its way towards the terrain surface. Along the fissure line lava fountains were estimated to have reached heights of 800-1400 m. The eruption rapidly became known in Iceland as the Skaftáreldur (the Skaftá river fires).

Henderson in 1818 publiced a vivid acount of the initial phases of the Laki eruption: *"From the 1st to the 8th of June, 1783, the inhabitants of West Skaftafell's Syssel were alarmed by repeated shocks of an earthquake, which, as they daily increased in violence, left no reason to doubt that some dreadful volcanic explosion was about to take place. Pitching tents in the open fields, they deserted their houses, and awaited, in awful suspense, the issue of these terrifying prognostics. On the morning of the 8th, a prodigious amount of dense smoke darkened the atmosphere, and was observed to be continually augmented by fresh columns arising from behind the low hills, along the southern base of which the farms constituting the parish of Sida, are situated….*

…. A strong south wind prevented the cloud from advancing over the farms; but the heath, or common, lying between them and the volcano, was completely covered with ashes, pumice, and brimstone. The eruption had now actually commenced; and the raging fire, as if sublimated into greater fury by the vent it had obtained, occasioned more dreadful tremefactions, accompanied by loud subterraneous reports, while the sulphureous substances that filled the air, breaking forth into flames, produced, as it were, one continued flash of lightning, with the most tremendous peals of thunder that were ever heard. The extreme degree to which the earth in the vicinity of the volcano was heated, melted an immense quantity of ice, and caused a great overflow in all the rivers originating in that quarter….

…. Upon the 10th, the flames first became visible. Vast fire-spouts were seen rushing up amid the volumes of smoke, and the torrent of lava that was thrown up, flowing in a south-west direction, through the valley called Ulfarsdal, till it reached the river Skaptá, when a violent contention between the two opposite elements ensued, attended with the escape of an amazing quantity of steam but the fiery current ultimately prevailed, and, forcing itself across the channel of the river, completely dried it up in less than twenty-four hours; so that, on the 11th, the Skaptá could be crossed in the low country on foot, at those places where it was only possible before to pass it in boats. The cause of its desiccation soon became apparent: for the lava, having collected in the channel, which lies between high rocks, and is in many places from 400 to 600 feet in depth, and near 200 in breadth, not only filled it up to the brink, but overflowed the adjacent fields to a considerable extent; and, pursuing the course of the river with great velocity, the dreadful torrent of red-hot melted matter approached the farms on both sides, greatly damaged those of Hvammur and Svinadal to the west, and that of Skaftárdal to the east….."

In total, the Laki eruption produced about 15 km^3 lava, which covered huge areas in southern Iceland. Most of the lava erupted during the first five months of the eruption. In addition, clouds volcanic ash and poisonous fluorine/sulphur-dioxide compounds were released around the eruption site, killing more than half of the Icelandic livestock.

The eruption ended on February 7, 1784. The Grímsvötn volcano, from which the Laki fissure extends, was also erupting at the time from 1783 until 1785.

The eruption of Laki was probably one of the most devastating events to occur in modern Icelandic history. Already greatly weakened by the harsh climate of the Little Ice Age, coupled with the rigours of exploitation under an uncaring and exploitative Danish trading monopoly, Iceland was little prepared to withstand the consequences of this natural disaster.

Mainly because of massive losses to livestock during and after the eruption, and later by starvation caused by the destruction of grasslands and home-fields by volcanic ash, the death-rate soared in the years immediately following the eruption. Prior to the eruption, the Icelandic population numbered about 50,000, and declined more than 10,000 following the eruption. According to a contemporary source (Nicol 1844), about 19,488 horses, 6801 horned cattle, and 129,937 sheep was lost in Iceland 1873-1885 because of the eruption.

It took about 40 years before the population was back to the pre-eruption level, and farms destroyed or abandoned were either reconstructed or re-inhabited. Many people decided to leave Iceland for good over the next century, emigrating to Canada, United States, and other countries.

Moss covered lava fields near Kirkjubæjarklaustur in southern Iceland, derived from the Laki 1783-1784 eruption. In the background the southern part of the ice cap Vatnajökull is seen. The highest summit is Öræfajökull (2109 m asl.), the highest active volcano in Iceland. It has erupted twice in historical time, in year 1362 and 1727. Photo taken September 16, 2003.

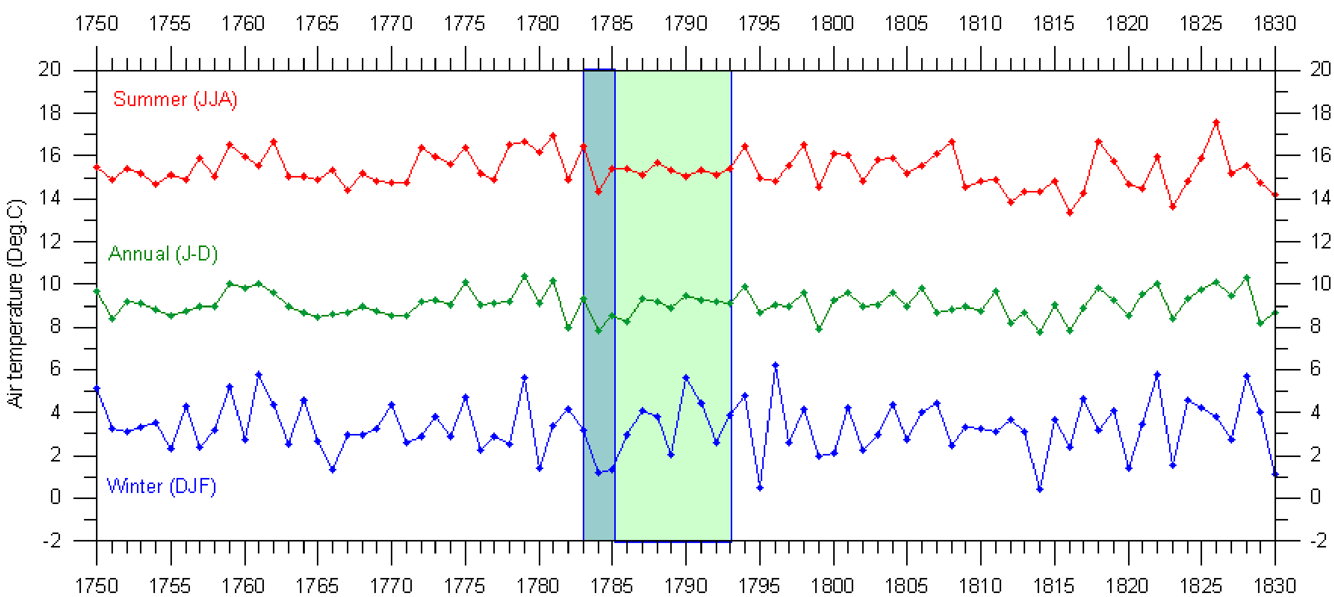

Central England temperature series 1750-1830. The length of the Laki-Grímsvötn 1783-1785 volcanic eruption is indicated by the dark blue bar. The immediate cooling effect of the eruption is clearly seen, both summer and winter. The bar 1785-1793 indicate a subsequent period with relatively low air temperatures recorded in Central England, especially during the growing season (summer). This period may at least partly be due to a higher atmospheric content of aerosols *in the years following the eruption. These graphs have been prepared using the composite monthly meteorological series since 1659, originally painstakingly homogenized and published by the late professor* Gordon Manley (1974)*. The data series is now updated by the Hadley Centre in UK and may be downloaded from there.*

The total volume of volcanic ash (tephra) produced by the Laki eruption has been estimated to more than 0.9 km^3. The summer of 1783 was warm and a rare high pressure zone located over Iceland caused the ash and poisonous gasses to be carried rapidly to the south-east, and ash therefore fell over large areas of Europe. The outpouring of gases, including 8 million tons of fluorine and 120 million tons of sulphur dioxide gave rise to what has since become known as the "Laki haze" across Europe. This sulphurous haze is reported to have caused thousands of deaths in Europe throughout 1783 and the winter of 1784. In Great Britain, the summer of 1783 was known as the "sand-summer" due to ash fallout, and it has been estimated that about 23,000 British people died from the poisoning in August and September 1783.

The gases and ash derived from the Laki eruption were carried by the convective eruption column to altitudes of about 15 km in the atmosphere, and the aerosols caused a significant cooling effect in the Northern Hemisphere, as is documented by the Central England meteorological record. The sulphur hazes may well have been the primary cause of the cooling that occurred after the large Laki 1783-1785 eruption.

In France, a sequence of meteorological extremes included a harvest in 1785 that caused poverty for rural workers, accompanied by droughts, bad winters and summers, including a violent hailstorm in 1788 that destroyed crops. This in turn contributed significantly to increasing poverty and famine that presumably contributed towards triggering the French Revolution in 1789. The growing season temperature in NW Europe was generally low in the years following the Laki eruption until 1794 (see graph above). In Norway, also in 1789, following a cold winter with deep frost penetration, heavy rainstorms 21-23 July resulted in numerous landslides and the largest historical Norwegian flood known, the Storofsen flood in July 1789.

In North America, the winter of 1784 was the longest and one of the coldest on record. It was the longest period of below-zero temperature in New England, the largest accumulation of snow in New Jersey, and the longest freezing over of Chesapeake Bay. There was ice skating in Charleston Harbour, a huge snowstorm hit the south, the Mississippi River froze at New Orleans, and there was ice in the Gulf of Mexico.

References:

Henderson, E. 1818. *Iceland: Or The Journal Of A Residence In That Island, During The Years 1814 And 1815.* Volume 1, pp. 276-289.

Manley, G. 1974. Central England Temperatures: monthly means 1659 to 1973. *Quaterly Journal of the Royal Meteorological Society 100*, 389-405.

Nicol, J. 1844. *An Historical and Descriptive Account of Iceland, Greenland, and the Faroe Islands*. pp. 199-200.

*****

All diagrams in this report, along with any supplementary information, including links to data sources and previous issues of this newsletter, are freely available for download on www.climate4you.com

Yours sincerely,

Ole Humlum (Ole.Humlum@geo.uio.no)

December 19, 2016.